The Islamic University of Gaza
Postgraduate Studies
Faculty of Engineering
Electrical Engineering Department

Design of compact Multiband Folded loop Antenna for MIMO applications

تصميم هوائي مدمج متعدد النطاقات الترددية من نوع حلقي مطوي الشكل للتطبيقات المتعددة الإدخال متعددة الإخراج

Submitted by:
ABDALWAHAB M. ALUTOL

Supervisors:

Dr. FADY EL NAHAL
Dr. MOSTAFA Abu NASER

A Thesis Submitted in Partial Fulfillment of the Requirements for the Degree of Master in Electrical Engineering/Communication Systems

May, 2014

DEDICATION

To my parents

Who taught me the value of study and perseverance ethic and have given me endless support

To my wife, sons and daughters

Who encouraged me through the work of this thesis

To my brothers and sisters

To my friends

ACKNOWLEDGMENTS

In the name of Allah S.W.T.

First of all, without the enlightenment of ALLAH, this work would not have been done successfully.

I would like to express my sincere thankfulness to my supervisors, Dr. Faddy El-Nahal and Dr. Mostafa Abu Naser, for their guidance and consistent support. Apart from their valuable academic advice and guidelines, they have been extremely kind, friendly, and helpful.

I would also like to thank the committee members, Dr. Talal Skaik and Dr. Abdel Hakeim Husein for their time in reviewing the thesis and for their care, cooperation and constructive advices.

Special thanks to all the friends for their constant support and encouragement through my study.

In the last I would like to thank my parents and family for their efforts, motivation, support and prayers. It has been only possible due to them.

ABSTRACT

Multiple input multiple output (MIMO) technology is one of the key techniques used in the next generation Wireless Communication, MIMO can either increase the transmission systems reliability by applying diversity or increase the achievable data rate by transmitting several spatially separated data streams in parallel. This thesis presents an implementation and performance evaluation of multiple antenna system using a compact folded loop antenna (FLA) covering LTE2600/WIMAX3.5/WLAN2.4/5.2 frequency bands for handheld devices.

First of all, a single element compact internal penta-band FLA is proposed on a ground plane of size equivalent to a handheld device. Parametric analysis study has been performed to get the required specifications and simulated results exhibit that for all the bands the proposed FLA features have nearly good omnidirectional radiation patterns with proper gain.

Next an implementation of MIMO configuration of the FLA was then studied. The MIMO antenna also designed to be suitable to a handheld devices form factor. The goal is to design a two element multiple antenna on the same ground plane with lower correlation values while keeping same operating bands and gain. Three different cases with different configurations of the two antenna placement on the ground plane has been designed to compare the results in terms of return loss, mutual coupling and correlation. The design and optimizing of the performance of the proposed antenna are performed by using a high frequency structure simulator HFSS.

The result meet all the required specification where the proposed design results maintaining a value of correlation coefficient below 0.5 over the frequency bands of operation and nearly 10 dB diversity gain are obtained.

ملخص الرسالة

تعتبر تقنية MIMO أحدى السمات الرئيسية لأنظمة الاتصالات اللاسلكية من الجيل القادم، تستطيع تقنية MIMO زيادة الثقة في انظمة الارسال وذلك باستخدام نظام التعددية أو زيادة معدل نقل البيانات عن طريق نقلها من خلال ارسال اكثر من سيل من البيانات المنفصلة مكانيا بشكل متوازي، تقدم هذه الاطروحة تصميم وتقييم لنظام متعدد الهوائيات باستخدام هوائي من نواع حلقي مطوي للعمل ضمن النطاق الترددي لانظمة الاتصالات LTE/2600/WIMAX3.5/WLAN2.4/5.2 و مناسبة للاجهزة المحمولة، بدايةً ، تم تصميم هوائي احادي خماسي التردد على شكل حلقي مطوي على لوحة ارضي ذات حجم مناسب للاجهزة المحمولة ، وتم اجراء تحليل للمتغيرات للوصول للمواصفات المطلوبة ،نتيجة المحاكاة اظهرت ان الهوائي الحلقي المقترح له مميزات جيدة بحيث نمط الاشعاع مشابه لمتعدد الاتجاهات وله كسب مناسب.

الخطوة الثانية ، تم تطبيق منظومة MIMO على الهوائي الحلقي المصمم وتم تصميمه ليكون مناسبا للاجهزة المحمولة ايضا، والهدف هو تصميم هوائي ثنائي على نفس لوحة الارضي ليحقق معامل تشابه منخفض ويحافظ على نفس نتائج النطاقات الترددية والكسب، وتم تصميم ثلاث نماذج للهوائي الثنائي لاماكن ترتيبها على لوحة الارضي ليتم مقارنة النتائج بين النماذج المختلفة حسب الخسارة الراجعة والازدواج المتبادل ومعاملات التشابه.

عملية التصميم والمحاكاة وتحقيق الأمثلية تمت باستخدام حزمة HFSS، والنتائج تتماشى مع المواصفات المطلوبة بحيث ان التصميم المقترح يحقق معادل تشابه أقل من 0.5 وكسب التنويع تقريبا يساوي 10 ديسيبل.

TABLE OF CONTENTS

Chapter 3: Multiple Antenna Systems

Chapter 4: Single Folded Loop Antenna Design

Chapter 5: MIMO Design Simulation

Chapter 6: Conclusion and Future Work

LIST OF TABELS

LIST OF FIGURES

LIST OF ABBREVIATIONS

3D: Three-Dimensional

3G: Third Generation

3GPP: Third Generation Partnership Project

4G: Fourth-Generation

ADG Apparent Diversity Gain

DG Diversity Gain

EDG Effective Diversity Gain

ECC: Envelope Correlation Coefficient

CDF: Cumulative Distribution Function

E field: Electric field

FEM: Finite Element Method

H field: Magnetic field

IEEE: Institute of Electrical and Electronics Engineers

ILA: Inverted-L Antenna

HAC: Hearing Aid Compatibility

HFSS: High Frequency Structure Simulator

LTE: Long Term Evolution

MIMO: Multi input multi output

MRC: Maximal Ratio Combining

PCB: Printed Circuit Board

PCS: Personal Communication Service

PIFA: Planar Inverted F Antenna

SAR: Specific Absorption Rate

SISO: Single Input Single Output

SNR: Signal to Noise Ratio

SWC: Switch Combining

UMTS: Universal Mobile Telecommunications System

WCDMA: Wide band Code Division Multiple Access

WiMAX: World Interoperability for Microwave Access

WLAN: Wireless Local Area Network

XPR: Cross-polar ratio

1

Introduction

1.1 Background

With the rapid evolution of wireless communication technologies, and the changing nature of consumer needs for mobile devices, mobile handsets have been gradually rising towards miniaturized, ultra-slim, highly integrated, multi-system and high-performance. Hence the demands for designing multi-band compact antennas to meet the growing desires of integrating more applications in close proximity inside the limited space of the mobile handsets are increased continuously. Furthermore, there are a lot of common services nowadays the customers would like to be in his terminals such as: Internet access, video streaming, games downloading files and etc. However, all these services require a higher data rate transmission than conventional voice calls. The world's leading companies in mobile communications have given a huge force to the development of 4G wireless systems to satisfy the customers' demand for high data rate, quality of transmission and accuracy. MIMO antenna system is a key feature enabling technology for fourth generation (4G) wireless communication [1]. This technology has become a good solution to fulfill the demand for high data rate and to improve the performance of future wireless communication systems [2]. This is primarily because MIMO systems can increase channel capacity with an increase in the number of antennas [3], without additional bandwidth or transmit power. MIMO is a key component of modern wireless communication standards, such as IEEE 802.11 (Wi-Fi), Third Generation Partnership Project (3GPP) Long Term Evolution (LTE) [4], and Worldwide Interoperability for Microwave Access (WiMAX) [5].

There are many wireless standard that are considered in a single wireless device. A mobile phone now can be used for talking, web browsing, file sharing, playing games online and using GPS and Bluetooth. Thus the mobile handheld device needs a multiband antennas can simultaneously operate in multiple frequencies, covering all the required wireless communication frequencies. Table 1.1 shows some common wireless communications bands [6].

Table 1.1. Common wireless communication frequency bands:

Applications Frequency range	Frequency Range
LTE 700MHz	746- 798
LTE 2.6GHz	2500-2700
Global System for Mobile Communications (GSM) 850MHz	824- 890
GSM 900	880- 960
Global Positioning System (GPS)	1557 , 1227
Industrial, Scientific and Medical (ISM) / Bluetooth 2.4GHz	2300- 2500
Worldwide Interoperability for Microwave Access (WiMAX)	3000 - 4000
Wireless Local Area Network (WLAN) 5 GHz	5100 -5800
Digital Cellular Service (DCS) 1800	1710-1880
Personal Communications Service (PCS) 1900	1850-1990
Code Division Multiple Access (CDMA) 2100	1920-2170

1.2 WLAN

Wireless Local Area Network (WLAN) is one of the most widely used technologies in today's communication world. It is one reliable and cost effective solution for wireless high speed data connectivity and viable solution for high-speed data connectivity, WLAN technology basics are specified in the IEEE 802.11 family of standards, the technology behind 802.11 is branded to consumers as Wireless Fidelity (Wi-Fi). The first two variants of 802.11 standard are IEEE 802.11b which operates frequency band, 2.4–2.484 GHz, and IEEE 802.11a, which operates in the available 5 GHz bands (5.15-5.35 GHz, 5.47-5.725 GHz, and 5.725-5.825 GHz). A third variant, IEEE 802.11g operates in 2.4 GHz band.

WLAN uses spread-spectrum or Orthogonal Frequency Division Multiplexing (OFDM) modulation technology based on radio waves that allows users to have a higher mobility and to transmit large amounts of digital data. OFDM technique splits the radio signal into multiple small signals and then transmits them simultaneously at different frequencies to the receiver. WLAN system is Time Division Duplex (TDD), where the same frequency is used for transmission and reception [7].

1.3 WIMAX

WiMAX technology is a Broadband Wireless Access (BWA) technology which offers greater range and bandwidth than Wi-Fi. It provides the BWA services as an alternative to the wired technologies like cable and digital subscriber line (DSL). There are some standards of WiMAX that are used for communication, IEEE 802.16d and IEEE 802.16e standards are commonly used. IEEE 802.16d is a fixed wireless technology adjusted for fixed and nomadic applications in line of sight (LOS) and non-line of sight (NLOS) environments. It uses orthogonal frequency division multiplexing (OFDM). 802.16e is a mobile WiMAX standard targeted for mobile application as well as fixed and nomadic applications in NLOS environments. Mobile WIMAX provides enhancements to WiMAX standard by giving users the ability to support subscriber stations moving at vehicular speeds. There is no uniform global licensed spectrum for WiMAX, although the WiMAX Forum has published three licensed spectrum profiles: 2.5 GHz (2.5 - 2.69 GHZ), 3.5GHz (3.4 -3.69 GHZ) and 5.5GHz (5.25-5.85 GHZ). WiMAX supports a wide variety of features including MIMO techniques, smart antenna technologies, time division duplex (TDD) and frequency division duplex (FDD) operating modes and a wide range of bandwidths. The WiMAX is able to implement the coverage of tens of kilometers and a peak data rate up to 74Mbps when operating with a 20 MHz bandwidth [7].

1.4 LTE

Long-term evolution (LTE) is a promising standard for next-generation wireless communication systems in various regions of the world to increase the capacity and speed of the mobile and other handheld terminals, The LTE system is based on OFDM and supports scalable bandwidth from 1.4 MHz to 20 MHz. The cell size of the LTE system can vary from tens of meters in radius to a hundred kilometers. The standard is expected to deliver a wireless data transfer rate of 300 Mb/s in the downstream and 75 Mb/s in the upstream. In order to achieve such a high mobile data rate, MIMO technology is employed in the LTE. There is a number of LTE frequency bands that are being designated for use with LTE. Some of these frequency bands are already in use for other mobile communication systems, whereas other LTE bands are new, frequency spectrum allocated for LTE applications ranges from 400 MHz to 4 GHz [8].

1.5 Problem Statement

It is widely known that the usage of MIMO has been shown to be highly advantageous. However, when multiple antennas are involved at closer spacing the technical challenges are more pronounced compared to a single antenna system. The acceptable antenna correlation for reliable MIMO performance for mobile terminals is reported to be < 0.5 [9]. The parameter that describes the correlation between the received signals in highly diversified environments is mutual coupling. Mutual coupling defines the electromagnetic interaction between antennas, it is intrinsic to the nature of antennas that when two antennas are in proximity and one is transmitting, the second will receive some of the transmitted energy, even if both antennas are transmitting, they will receive part of each other's transmitted energy. Furthermore, antennas re-scatter a portion of any incident wave and thus act like small transmitters even when they are nominally only receiving. The result is that energy interchange between a certain element of a multiple antenna system and a remote point occurs not only by the direct path, but also indirectly via scattering from the other antennas of the multiple system. Higher mutual coupling may result in higher correlation coefficients thus reducing the antenna efficiencies. The mutual coupling mainly depends on the distance between the elements of an antennas, by increasing the distance between the elements of the antennas, the mutual coupling can be reduced. However, the distance between the antennas cannot be maintained too large, since MIMO systems have their major applications in mobile terminals, for example in handheld devices the antenna correlation is inherently high as closely packed antennas are strongly coupled to each other.

In this thesis a multiple-element FLA for mobile terminal having good diversity performance and low mutual coupling between the antenna elements is proposed and investigated so as to improve the reliability and capacity of MIMO systems. The covered frequency bands that will be studied are LTE (2.6 GHz), WIMAX (3.5 GHz) and WLAN (2.4, 5.2 and 5.8 GHz). As specifications for this thesis, both of them must have a return loss better than 6 dB, radiation efficiency higher than 50% and a correlation coefficient between the two antennas approximately of 0.5 and diversity gain around 10 dB.

1.6 Literature Review

In order to start the thesis, the first step is to study the research completed by other researchers in the field on the topic. With the help of literature review, it becomes clearer to build from previous knowledge and to perform this project.

In [10] the design of a compact internal folded loop antenna for GSM850/900, DCS, PCS, UMTS, LTE2300/2500, WLAN2.4GHz and WiMAX2.5GHz multiple mobile communication systems has been presented. A continuous meander line shape folded loop radiating path and a T-shape coupling element on the back plane of the PCB are used in the design. In another multiband design [11], an internal hexa-band folded monopole/dipole/loop antenna for mobile communication systems has been proposed, the proposed antenna has four resonances, 0.5λ, 1λ, 1.5 λ and 2 λ modes, all of these four modes can thus be utilized to cover cellular bands including the LTE700, GSM850/900, GSM1850/1900, and UMTS2100. A surface-mount antenna formed by folding a dual-loop metallic strip onto a foam base has been proposed in [12], for achieving dual-frequency operation covering the 2.4 GHz (2400–2484 MHz) and 5 GHz (5150–5350 and 5725–5875 MHz) WLAN bands. A simple printed-loop antenna with wideband characteristics is presented for laptop applications in [13]. This design shows multiband and four resonant modes below 4 GHz. U-shaped tuning element printed on the back side of the circuit board adjusts the resonant modes to cover GSM850, GSM900, DCS, PCS, UMTS, WLAN and WiMAX bands. In addition, a single element multiband folded loop antenna cover five-band characteristics for smart phone applications is proposed in [14].

All the above researches only studied single element antenna design. The following works deal with MIMO antenna configuration. In [15] a compact dual-band dual-port system for handheld devices has been proposed. The proposed antenna operates in two frequency bands, 790-862 MHz and 2500-2690 MHz, thereby making it suitable for LTE handheld devices. In [16] a dual-loop antenna design applied to a three-antenna system suitable to be concealed inside wireless access points for MIMO applications in the WLAN 2.4/5.2/5.8 GHz bands is presented. In [17] a compact planar MIMO antenna system of four elements with similar radiation characteristics is proposed for the whole 2.4-GHz WLAN band. Two types of antenna elements printed on different sides of the substrate are used in the structure for better isolation performance.

1.7 Simulation Tool

Ansoft HFSS is used for full wave analysis of the multiband antenna model. HFSS is a 3D electromagnetic field simulator for high frequency and high speed components, HFSS can be used to simulate and analyze any 3D passive elements such as the slots, horns, linear wires, patch antennas and other microwave passive components. Also lumped circuit components can be simulated. HFSS uses discrete, fast, interpolating sweep types. Typically discrete sweep requires more memory to produce accurate results as compared fast sweep. Electromagnetic fields Maxwell's Equations are solved using Finite Element Method (FEM). HFSS divides the entire structure into a large number of small regions called tetrahedron. For a structure with excitation ports, HFSS assumes that each port is connected to a uniform waveguide with the same cross section as the port. HFSS computes the electric fields for each mode that the port supports and then generate S matrix from the amount of the reflection and transmission through the port. An adaptive mesh operation is utilized to generate the accurate mesh for the structure. Also meshing can be given manually. Generally the mesh size is kept as lambda by 10 for the highest frequency of frequency sweep. It uses an iterative process to optimize the mesh until the difference in S parameters between the current iteration and last iteration (delta S) converges below the value specified by the user (mostly <0.02). The accuracy of results can be less if proper meshing is not defined. The results are then checked to fulfill the requirements of the specification [18]. Figure 1.1 shows a picture of a calculated mesh in HFSS for the proposed antenna design, it's noticed that the mesh structure is thicker in the areas with finer detail.

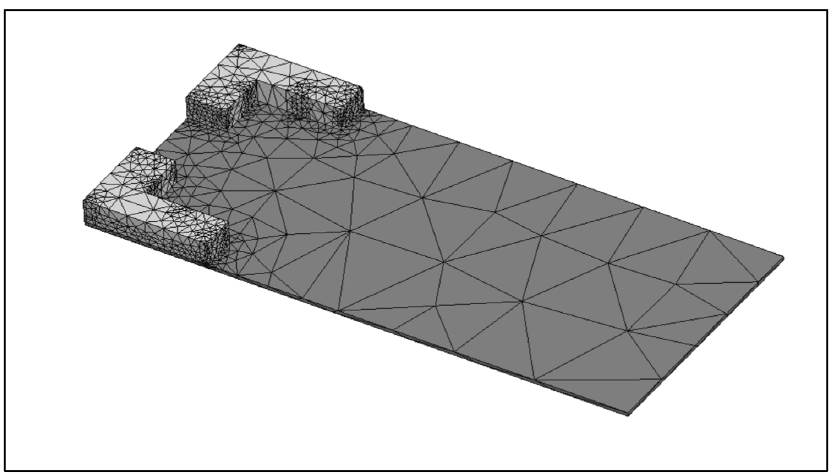

Figure 1.1. A mesh for FEM calculations with HFSS.

1.8 Objectives of the thesis

There are many objectives of this thesis; these objectives are presented as the following:

- Designing a compact antenna for handheld devices running MIMO applications, the design cover operating frequency of LTE (2.6 GHz), WLAN (2.4/5.2/5.8GHz) and WIMAX (3.5GHz), the size of the antenna should be suitable for commercial smartphone handset devices.
- Comparing and comment on the simulated obtained reflection and radiation responses of the antenna.
- Try to evaluate the performance of MIMO systems, by assessment of MIMO system performance metric like antenna correlation, matching efficiency.

1.9 Outlines of the thesis

The thesis is divided into six chapters as detailed below:

Chapter 2 introduces a background on the antenna basics, the Maxwell's equations and the radiation pattern of antenna. Antenna parameters such as return loss, input impedance, bandwidth, directivity, antenna efficiency, gain and polarization are also discussed.

Chapter 3 provides basic theoretical concepts and background related with the multiple antenna systems, two different types of coding schemes that can be used to exploit the MIMO channels are addressed. Three relevant metrics and their calculations for diversity performance are described: Envelope correlation coefficient, embedded efficiency and diversity gain.

Chapter 4 presents single element FLA design, simulated results are shown for the reflection coefficient, peak realized gain, 2D/3D radiation patterns and current distributions.

Chapter 5 introduces a deployment of MIMO configuration of the single element antenna designed in Chapter 4, a study of three cases of antenna placement on the ground plane are introduced, simulated results are shown for the reflection coefficient, mutual coupling, peak realized gain, efficiency, total antenna efficiency, envelope correlation coefficient, diversity gain, 2D/3D radiation patterns and current distributions are investigated.

Chapter 6 presents the conclusion of the research, and the suggestions for future work.

2

Antenna Theory

2.1 Introduction

Antenna is a major component of a wireless communication system. An antenna is a passive device used to transform an RF signal, traveling on a conductor, into an electromagnetic (EM) guided wave in free space and vice versa [19]. This process is explained by a general communication between a transmitting antenna and a receiving antenna, as described in Figure 2.1 [20]. Antennas demonstrate a property known as reciprocity, which means that an antenna will maintain the same characteristics regardless if it works as transmitter or receiver.

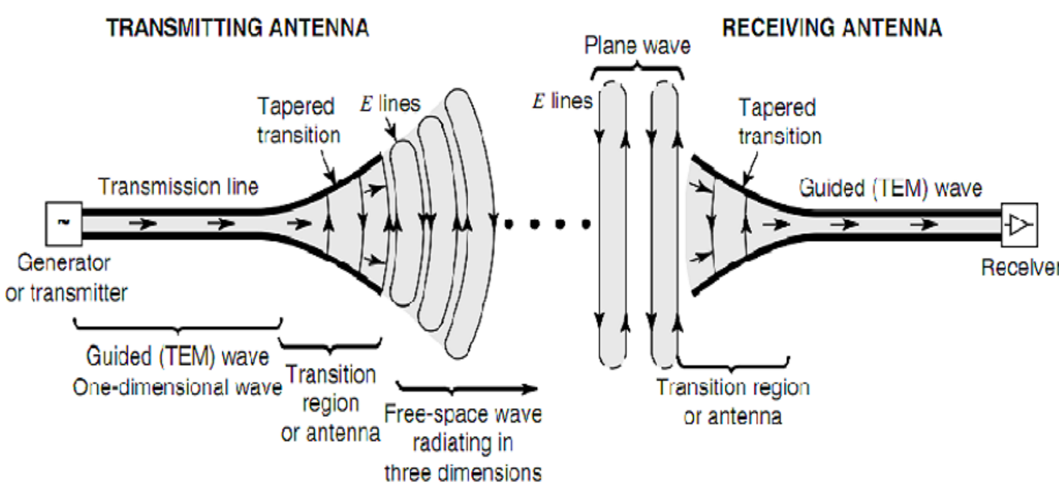

Figure 2.1. The antenna as a transition structure, for a transmitting antenna and for a receiving antenna.

Antennas are frequency-dependent devices. Since each antenna is designed to operate in a certain frequency band and reject signals the other operating band, antennas can be considered as a band pass filters. The electromagnetic behavior and the operation of antennas can be described by Maxwell's equations [21].

$$\nabla \times \vec{E} = \frac{-\partial \vec{B}}{\partial t} \tag{2.1}$$

$$\nabla \times \vec{H} = \frac{-\partial \vec{D}}{\partial t} + \vec{J} \tag{2.2}$$

$$\nabla \cdot \vec{D} = \rho \tag{2.3}$$

$$\nabla \cdot \vec{B} = 0 \tag{2.4}$$

where $\vec{E}$ is the electric field intensity, $\vec{H}$ is the magnetic field intensity, $\vec{D}$ is the electric flux density, $\vec{B}$ is the magnetic flux density , $\vec{J}$ is the electric current density , ρ is the electric charge density, (.) is the dot-product vector operator, (×) is the cross-product vector operator, (∇) is the del vector differential operator.

2.2 Fundamental Parameters of Antenna

Antenna parameters are used to characterize performance of an antenna when designing and measuring antennas. The most fundamental antenna parameters such as radiation pattern, gain, input impedance, bandwidth and polarization are explained.

2.2.1 Radiation Pattern

Antenna radiation pattern is one of the most common parameter of antenna, according to IEEE Standard Definitions of Terms for Antennas, antenna radiation pattern is defined as: "A mathematical function or a graphical representation of the radiation properties of the antenna as the function of space coordinates. In most cases, the radiation pattern is determined in far-field region and is represented as a function of the directional coordinates. Radiation properties include power flux density, radiation intensity, field strength, directivity phase or polarization" [22]. Radiation pattern in the region close to the antenna is not as same as the pattern at large distances. The term near-field refers to the field pattern that exists close to the antenna, while the term far-field refers to the field pattern at large distances.

Based on the standard coordinate system, two geometrical principal planes can be defined: azimuth and elevation plane. The azimuth plane is defined as the plane in which the radiation pattern varies as a function of ϕ when $\theta = \pi/2$; the elevation plane is defined as the plane in which the radiation pattern varies as a function of θ, when ϕ is constant. Radiation patterns of antennas can be classified based on the pattern shape into isotropic, omnidirectional or directional patterns. The isotropic antenna radiates equally in all directions. The antenna radiates and receives equally in a given plane is called an omnidirectional antenna, and it is also called a non-directional antenna because it does not favor any particular direction in this plane. The directional antennas focus the energy more in a particular direction than in others [23].

2.2.2 Directivity

The directivity $D(\theta, \phi)$ of an antenna is a measure that describes how well the antenna directs the radiated energy. Directivity is defined as: "the ratio of the radiation intensity (U) in a given direction from the antenna to the radiation intensity averaged over all directions". The average radiation intensity is equal to the total power radiated by the antenna (P_{rad}) divided by 4π. Directivity can be expressed as [24]:

$$D(\theta, \phi) = \frac{4\pi U(\theta, \phi)}{P_{rad}} \tag{2.5}$$

2.2.3 Antenna Gain

The term antenna gain $G(\theta, \phi)$ describes how much power is transmitted in the direction of peak radiation to that of an isotropic source [22]. It can be defined as: "the ratio of the intensity, in a given direction, to the radiation intensity that would be obtained if the power accepted by the antenna were radiated isotropically". Mathematically Antenna gain is computed as follows [22]:

$$G(\theta, \phi) = \frac{4\pi U(\theta, \phi)}{P_{accepted}} \tag{2.6}$$

where $P_{accepted}$ is the net accepted power by the antenna. In most cases, the gain is relative, which is defined as the ratio of the power gain in a given direction to the power gain of a reference antenna in its referenced direction. The reference antenna is usually a dipole or isotropic antenna [25].

2.2.4 Input Impedance

Antenna input impedance is defined as the ratio of voltage to current at the antenna's terminals. To achieve maximum energy transfer the input impedance of the antenna must identically match the characteristic impedance of the transmission line. If the two impedances do not match, a reflected wave will be generated at the antenna terminal and travel back towards the source. This reflection of energy results in a reduction in the overall antenna efficiency. The impedance of an antenna is presented as the real (R) and reactive part (X) seen at the port of the antenna. The input impedance of an antenna is generally a function of frequency (ω). The impedance of an antenna, with no load attached, is defined as:

$$Z(\omega)=R(\omega)+jX(\omega) \tag{2.7}$$

2.2.5 Return Loss (RL)

Return loss (RL) is an important parameter when connecting an antenna. RL is a parameter which indicates the amount of power that is "lost" to the load and does not return as a reflection. RL is expressed as the ratio between incident power (Pin) and reflected power (Pr) expressed in dB, The RL is given by: [23]

$$RL = 10\log_{10}\left(\frac{P_{in}}{P_r}\right) \quad \text{(dB)} \tag{2.8}$$

RL evaluated at different frequencies of an antenna usually give a good representation of its radiating properties. For example, if RL= 0 dB, it means that the antenna isn't radiating at that frequency and RL= -20 dB or lower, it means that at least 99% of power either is radiated or absorbed inside the antenna.

2.2.6 Bandwidth

Bandwidth (BW) is a fundamental antenna parameter, BW is defined as "the range of usable frequencies within which the performance of the antenna, with respect to some characteristic, conforms to a specified standard." [23], the BW can be the range of frequencies on either side of the center frequency where the antenna characteristics like input impedance, radiation pattern, beam-width, polarization, gain, are close to those values which have been obtained at the center frequency.

2.2.7 Polarization

Polarization of a radiated wave is defined as "the property of an electromagnetic wave describing the time varying direction and relative magnitude of the electric field vector" [23]. It is described by the geometric figure traced by the electric field vector upon a stationary plane perpendicular to the direction of propagation, as the wave travels through that plane. The most common types of polarization include the linear (horizontal or vertical) and circular (right hand polarization or the left hand polarization) shown in Figure 2.2. Linear polarization is the simplest forms of antenna polarization. Circular polarization occurs when two or more linearly polarized waves add together, such that the E-field of the net wave rotates. Another form of polarization is known as elliptical polarization. It occurs when there is a mix of linear and circular polarization.

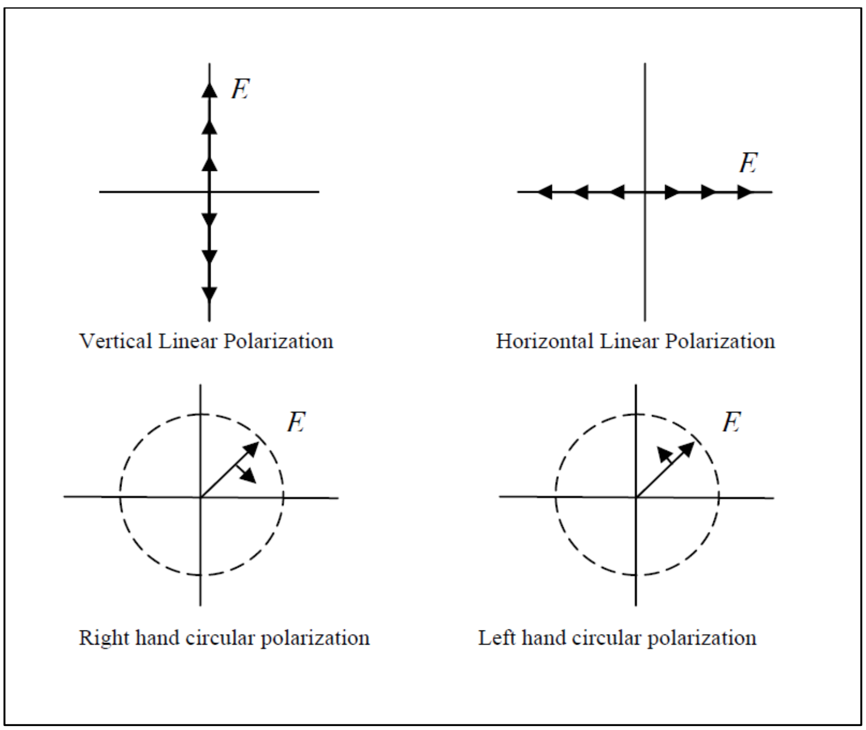

Figure 2.2. Commonly used polarization schemes

2.3 Types of antennas

In the past few years, many varieties of antenna systems for mobile terminals have been developed and used. These antennas include: monopole, Inverted-L Antenna (ILA) and

Inverted-F Antenna (IFA), planar inverted-F antenna (PIFA), microstrip patch and loop antenna. Some examples of antennas and their structures are summarized in this section.

2.3.1 Monopole Antennas

Monopole is an antenna with a quarter wavelength long consisting of vertical straight-wire radiator, mounted on a conducting ground plane, is shown in Figure 2.3 [26]. It is easy to design, light weight, and has omni-directional radiation pattern in the horizontal plane which has made it widely employed in cellular phone handsets. As the physical length of a monopole antenna is quarter of its wavelength at the operating frequency, this antenna is relatively very long, therefore monopole antennas are usually external antennas.

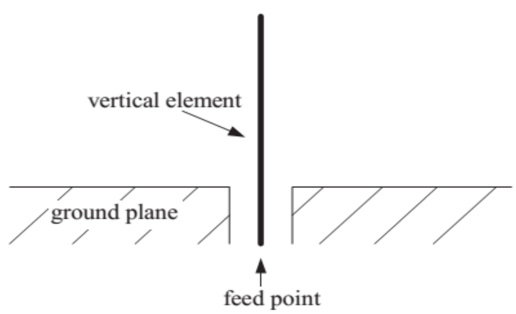

Figure 2.3. Monopole antenna.

2.3.2 ILA and IFA Antennas

An inverted-L antenna (ILA) consists of a short monopole as a vertical element and a wire horizontal element attached at the end of the monopole as shown in Figure 2.4. ILA was found to be a promising alternative to replace the external monopole antenna. The design of the ILA has a simple layout making it cost efficient to manufacture. It is a low profile antenna as the height of the vertical element is usually much less than a wavelength. The horizontal element normally has a length of about a quarter wavelengths.

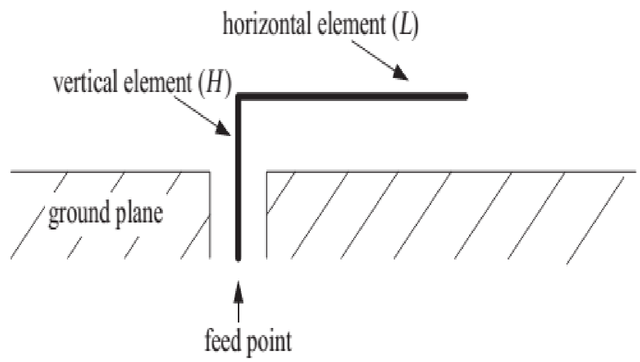

Figure 2.4. Inverted-L antenna (ILA)

The Inverted F Antenna (IFA) shown in Figure 2.5 typically consists of a rectangular planar element located above a ground plane, a short circuiting plate or pin, and a feeding mechanism for the planar element. The Inverted F antenna is a variant of the monopole where the top section has been folded down so as to be parallel with the ground plane.

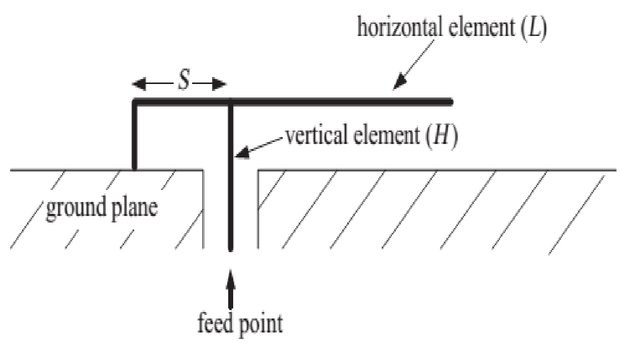

Figure 2.5. Inverted-F antenna (IFA)

2.3.3 PIFA Antenna

The PIFA antenna can be described as the modification of the IFA antenna. It can be achieved by replacing the radiating linear horizontal strip of the IFA antenna and replace it with a planar plate which is often placed parallel to the ground plane as shown in figure 2.6. This type of antenna is a variant of the patch antenna. It is very popular because of its low profile, omni-directional pattern, very high radiation efficiency and sufficient bandwidth in a compact antenna.

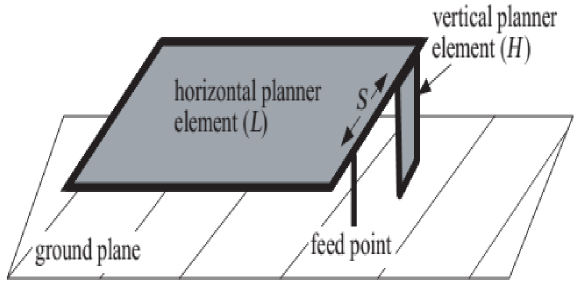

Figure 2.6. PIFA antenna

2.3.4 Microstrip Patch Antenna

microstrip patch antennas are usually very cheap and small. Microstrip patch antenna consists of a radiating metallic patch with a rectangular or circular shape on one side of a dielectric material substrate which has a ground plane on the other side as shown in Figure 2.7. Different feed configurations, including aperture coupled, microstrip line feed and coaxial feed can be used to microstrip antenna.

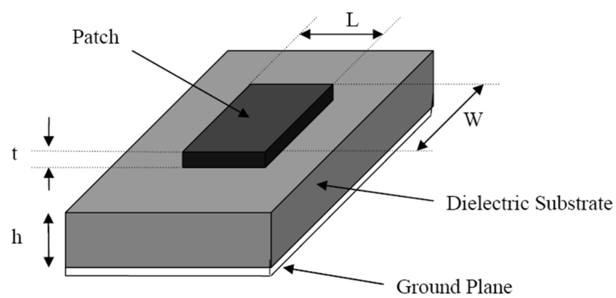

Figure 2.7. Structure of a Microstrip Patch Antenna

2.3.5 Loop Antenna

Loop antennas are characterized by closed current paths build on radiating elements, which comply with a variety of closed planar geometries. Loop antennas can be employed by directly printing on the mobile's phone board, or printing on a dielectric carrier and then mounted above the system circuit board [27, 28], or it can be can be also configured to be attached as a chip antenna as a surface-mountable on the system circuit board [29]. The characteristics of PIFA and IFA depend on the ground plane of the antenna as it used as part of the radiator thereby improve the bandwidth and gain performance [30, 31]. However, the current variation due to the device being handheld the resulting body proximity impact reduce antenna performance since the resonating currents are spread out over the system ground plane [32, 33]. It has been shown that the FLA antenna can decrease the currents on the ground plane significantly at the same time maintaining a good performance [34, 35].

These all make loop antenna very attractive for the publishers and applications of new mobile phone antenna projects. However, unlike the conventional mobile phone antennas such as (PIFAs) operated as quarter-wavelength resonant structures, the first resonant mode of the reported multiband loop antennas for mobile phone applications is a half-wavelength resonant mode. This makes it a challenge for reaching a compact volume for the loop antenna to be inserted inside the mobile phone as an internal antenna [36].

2.4 Summary

In this chapter an introduction and background of the antenna basics are introduced, the Maxwell's equations are also presented in this chapter. The antenna parameters such as return loss, input impedance, bandwidth, directivity, gain and polarization are discussed. Some examples of antenna systems for mobile terminals such as monopole, Inverted-L Antenna (ILA), Inverted-F Antenna (IFA), planar inverted-F antenna (PIFA) and loop antenna are discussed in this chapter.

3

Multiple Antenna Systems

3.1 Introduction

In a conventional wireless communication system, there is only one antenna at Transmitter and one at the receiver. This system which is called single input single output (SISO) system suffers from severe attenuation due to the destructive addition of multiple paths in the propagation media and due to interference from other users, results in a bottleneck in terms of capacity due to the Shannon-Nyquist criterion.

In order to increase the capacity of the SISO systems to meet the future wireless mobile services demand, the bandwidth and transmission power have to be increased significantly. Using multiple antennas systems the capacity of wireless communication system will increase substantially without increasing the transmission power and bandwidth [2].

Multiple antennas can be used to reduce the error rate as well as, improve the quality and capacity of a wireless transmission by directing the radiation only to the intended direction and adjusting the radiation according to the traffic condition and signal environment. Multiple antenna techniques are divided into two main categories, MIMO systems and diversity schemes.

3.2 MIMO Antenna Systems

The fundamental of MIMO systems is to take advantage of multi-path scattering, each pair of transmitting and receiving antennas provides a path for the signal from the transmitter to the receiver. By sending signals with the same frequency and the same information through different paths, multiple independent replicas of the data can be obtained at the receiver; hence, more reliable reception is achieved MIMO system could exploit the multipath fading to increase the capacity [37].

MIMO system can increase not only the channel capacity, but also the reliability of the wireless system can be enhanced by exploiting a coding schemes. The typical coding schemes of MIMO systems are spatial multiplexing and space time coding.

3.2.1 Spatial Multiplexing:

In spatial multiplexing technique, different data streams are transmitted simultaneously through several independent (spatial) communication channels by multiple antennas and at the same time the receiving side also use multiple antennas for receiving signals as shown in Figure 3.1. The amount of separation between the different data streams depends on the channel of propagation. If the signals arrive at the receiver antenna array with sufficiently different spatial signatures, the receiver can separate these streams into parallel channels thus improving the capacity. Spatial multiplexing is a very powerful technique for increasing channel capacity at higher signal to noise ratio (SNR). Spatial multiplexing can be used without knowledge of channel state information (CSI) at the transmitter. If the number of elements at the transmitter and the receiver are not equal, the maximum parallel channels that can be achieved in an ideal MIMO system is limited by the lesser in the number of antennas at the transmitter or receiver [38].

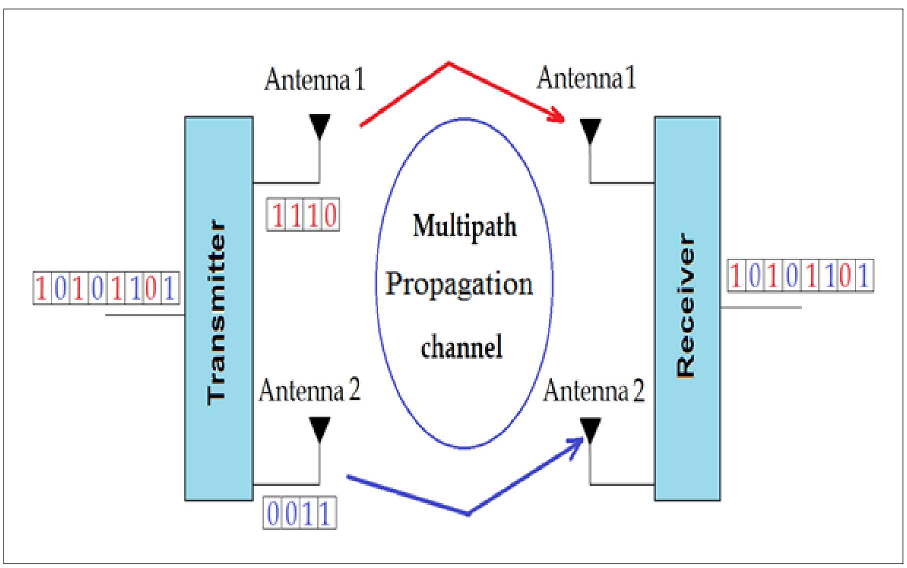

Figure 3.1. Spatial multiplexing block diagram

3.2.2 Space time coding

An alternative method of exploiting MIMO channels known as space-time coding, this method aims to improve the system's performance by exploiting the multiple element antennas for diversity gain rather than for the spatial-multiplexing gain of parallel data streams. In this methods, a single stream is transmitted, but the signal is encoded across both time and space to produce the symbol streams for each transmit element as shown in Figure 3.2. Appropriate decoding at the receiver is used to determine the best stream quality. This method is attractive as the system doesn't need to have information about the channel of propagation at the transmitter. The resulting diversity gain improves the reliability of fading wireless links and hence improves the quality of the transmission [39].

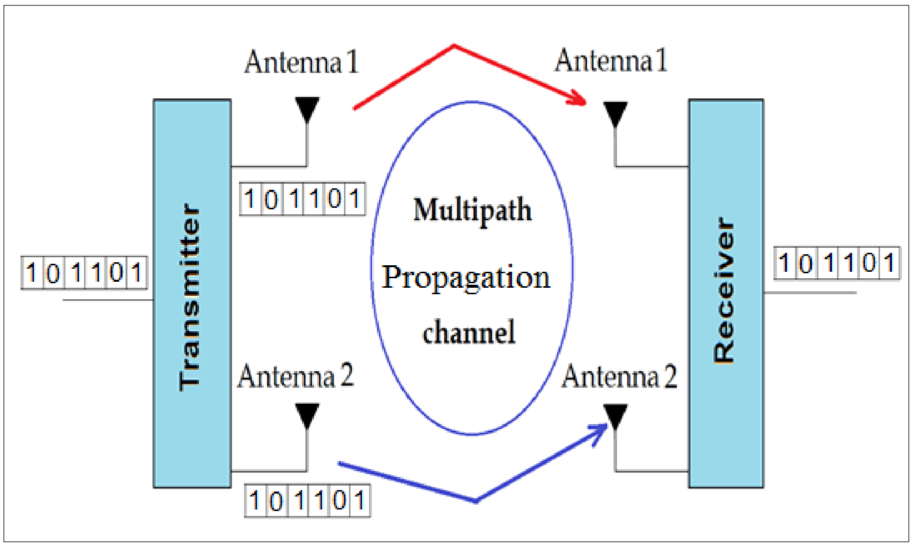

Figure 3.2. Space time coding block diagram.

3.2.3 System Model:

Figure 3.3 shows the block diagram of MIMO system consists of *M* transmit antennas and *N* receive antennas, each antenna received the direct component belong for it in addition the indirect components for the other antennas. The direct link from antenna 1 to 1 is specified with h11, etc., while the indirect connection from antenna 1 to 2 is identified as cross component h21, etc. The linear link model between transmit and receive antennas can be represented in the vector notations as:

$$y = H_x + n \tag{3.1}$$

Where y is the received signal vector, $y = [y_1 \ y_2 \ .... \ y_M]^T$, the superscript T stands for matrix transpose. x is transmitted signal vector, $x = [x_1 \ x_2 \ .... \ x_M]^T$. n is the N x 1 complex additive white Gaussian noise (AWGN) vector with zero mean and equal

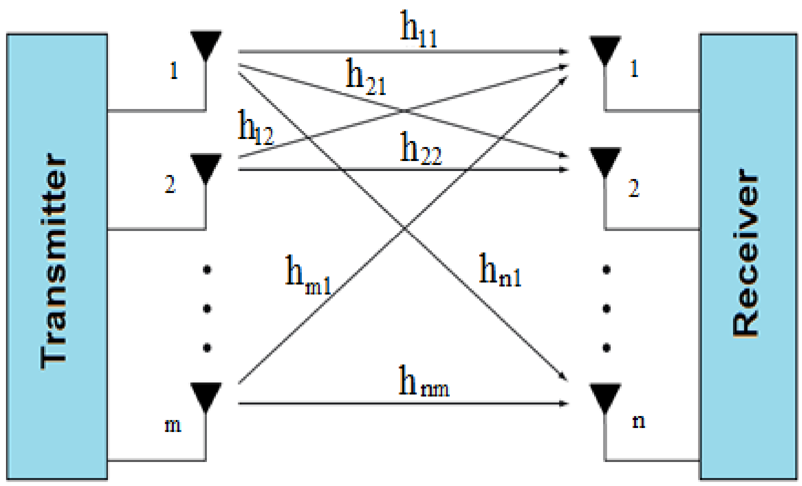

Figure 3.3. MIMO system diagram

variance, H is the $M \times N$ narrowband channel transfer matrix, which can be represented as:

$$H = \begin{bmatrix} h_{11} & h_{12} & \dots & h_{1M} \\ h_{21} & h_{22} & \dots & h_{2M} \\ \vdots & \vdots & \ddots & \vdots \\ h_{N1} & h_{N2} & \dots & h_{NM} \end{bmatrix} \quad (3.2)$$

H consist of elements H_{ij}, these elements are related to the multipath and scattering characteristics which get the information about magnitude and the phase of the distinct propagation paths also H also contains information about the antenna parameters [40].

$$H_{ij} = \lambda \sqrt{\frac{Zjt}{Zir}} \sqrt{\frac{R(Zir)}{R(Zjt)}} \sum_{p=1}^{P} (Fir((\theta,\Theta)ip)\, \Gamma ijpFjt((\theta,\Theta)jp) \quad (3.11)$$

where (Θ,θ)ip and (Θ θ)jp are the directions of the multipath components. Zjt and Zir are the characteristics reference impedance of the jth transmit and ith receiver port. The F terms are the normalized far field radiation patterns associated with the jth transmit and ith receive ports, respectively. Γijp is the polarimetric transfer matrix containing the information about polarization gain and phase. Also the elements of this matrix contains information of the free space propagation loss term, and other loses due to reflection, diffraction or scattering with objects present in the channel [40].

3.2.4 Capacity of MIMO system

Assuming that a MIMO system including the same number M of transmitting and receiving antennas, with no CSI at the transmitter and assuming that the transmitted signals are Gaussian distributed with identity covariance matrix and the received signals add coherently at the receiver, the capacity of a MIMO system is given by [41]:

$$C = log_2[\det\left(I_M \ + \frac{\gamma}{M} \ \mathrm{HH^H}\right)] \tag{3.3}$$

where I_M means M × M identity matrix, γ is the mean SNR at each receiver, det (.) means determinant and $(.)^H$ the Hermitian (complex conjugate transpose) of a matrix. The units of capacity are bits per second or Hertz (bits/s, bps/Hz).

3.3 Antenna Diversity Scheme:

Antenna diversity is a technique by which how multiple antennas are arranged to receive the independent multiple signals uncorrelatedly, and how multipath signals are combined to mitigate fading and improve the overall quality of the radio link, The basic principle of diversity is that the receiver combines multiple copies of the same signal arriving at the receiver, as the received signals will not go through the same deep fading simultaneously, and hence higher SNR are achieved. Figure 3.4 [42] shows the reception from two antennas subjected to the same multipath components. If the two multipath fading signals are uncorrelated, it is rare that both will be in a deep null at the same time. It is shown that the combined signal has a higher mean SNR at the output when compared to a single branch [43].

For antenna diversity techniques to be successfully realized in a wireless fading environment, two conditions have to be met: the multiple received signals must be uncorrelated, and the method that the signals is combined must defined.

3.4 Antenna Diversity Classifications

To achieve uncorrelated signals obtained by using multiple antennas system there are five approaches of diversities, i.e. frequency diversity, time diversity, spatial diversity, pattern diversity and polarization diversity. Among the five types of diversities, only the spatial, pattern and polarization diversity techniques are categorized as antenna diversity and they are described further in detail below [44].

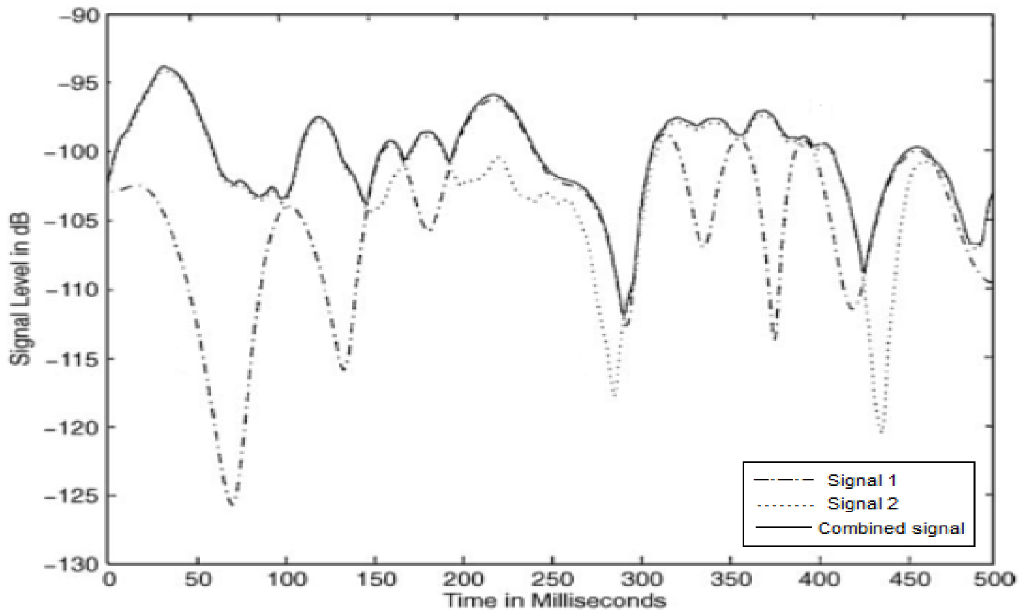

Figure 3.4. Two individually received signals and combined of the two signals by diversity technique.

3.4.1 Spatial Diversity

Spatial diversity is the most widely and simple diversity technique in wireless communication, It employs multiple antennas separated by certain spacing between them to get independent fading paths to achieve a space diversity antenna, the requirements of necessary space separation to obtain two uncorrelated signals, are applied to the mobile unit and the base station.

3.4.2 Pattern Diversity

Antenna pattern diversity produced by combining the signals of two antennas in such a way that two different antenna patterns occur, where the independent paths coming from different angles with different radiation patterns of different antennas can be detected simultaneously. In most cases, an array with appropriate beam switching is used at either transmitter, or receiver, this type of diversity is more effective in situation if antennas are enough spaced and adequately polarized. [45].

3.4.3 Polarization Diversity

In polarization diversity , different propagation characteristics of the vertically and horizontally polarized electromagnetic waves is utilized to provide two independent signal fades because they have quite different reflection behavior due to the nature of the polarized signals. In this diversity scheme, polarized antennas are required, polarization diversity does not require a large antenna separation to achieve its diversity gain. Polarization diversity can be implemented at the mobile station as well as at the base station [46].

3.5 Combining Methods

Diversity combining is the next important issue to be considered in diversity technology. There are four common diversity combining methods to combine the multiple received signals: switched combining, selection combining, equal gain combining and maximum ratio combining.

3.5.1 Switching Combining

The switched combining technique requires only one receiver frontend radio between the *N* branches as shown in Figure 3.5. A signal is chosen to receive when it is higher than the predefined threshold value. The receiver remains with the signal until the signal falls below the threshold value. Then the receiver switches to another signal that is higher than the threshold. Other combining techniques require N receivers to monitor the received instantaneous signals level of every branch when there are N element antennas while switching combing does not require monitoring of the other signals as long as the receiving signal is above the threshold level. Simplicity of switched combining makes it suitable to be implemented in mobile terminals [47].

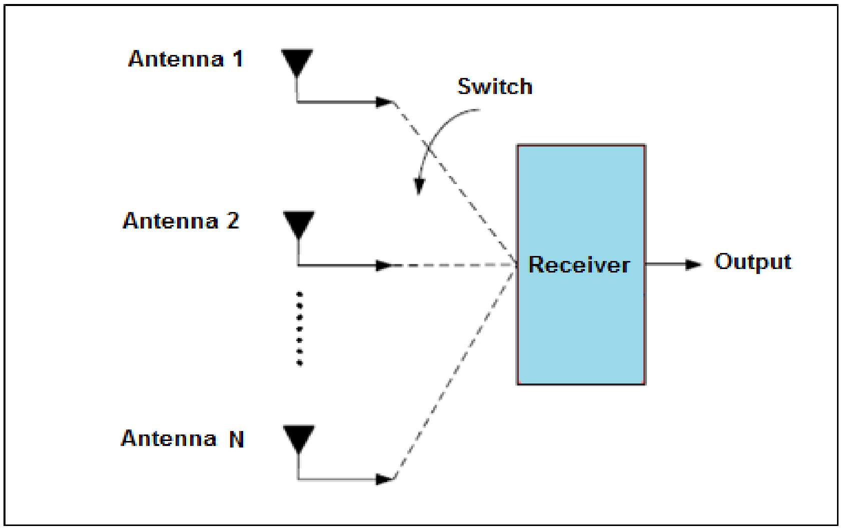

Figure 3.5. Block diagram of switched combining

3.5.2 Selection Combining

The selection combining technique is similar to the switched combining technique except that N receivers are required to monitor instantaneous SNR at all branches, the signal from that receiver which has the largest SNR is selected as the output signal as shown in figure 3.6.

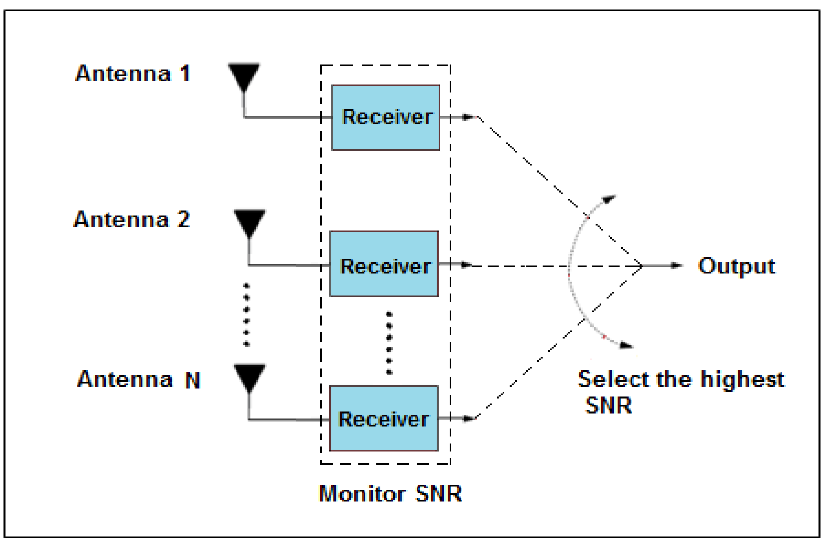

Figure 3.6. Block diagram of selection combining.

3.5.3 Equal Gain Combining

Since both switched and selection combining techniques only exploit the signal from one of the branches as the output signal at any given time, the signal energy in the other branches is wasted. In order to improve on this, the signals from all branches can be combined. Equal gain combining is a co-phase combining that brings all phases to a common point and combines them, the combined signal is simply the sum of the instantaneous fading envelopes of the individual branches as shown in figure 3.7, when this is achieved all signals will have zero phase and are combined coherently. Since no weight computation is required in equal gain combining the circuit for equal gain combining is relatively simple, it is usually used at the base station [47.48].

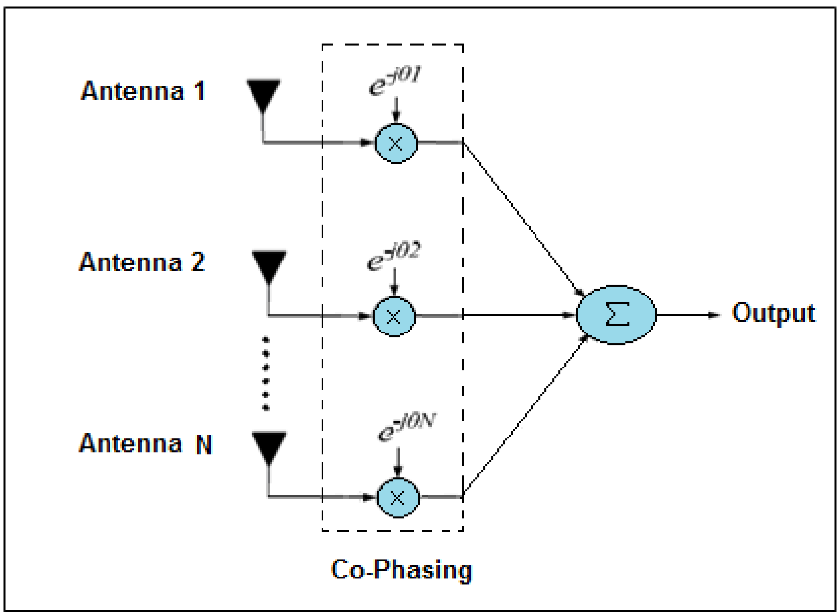

Figure 3.7. Block diagram of equal gain combining.

3.5.4 Maximum Ratio Combining

In the equal gain combining technique, all the branches may not have a similar SNR. Sometimes one of the branches has a much lower SNR than the other branches and this will reduce the overall SNR to a lower value at the output, Figure 3.8 shows the block diagram of maximum ratio combining, proper weights are assigned to each branch before all the signals are combined coherently which can maximize the signal-to-noise ratio of the sum of the received signals, a branch with a higher SNR will be given a higher weighting [49]. MRC gives the best performance to overcome the fading problem, but often at much greater cost and complication than other diversity techniques.

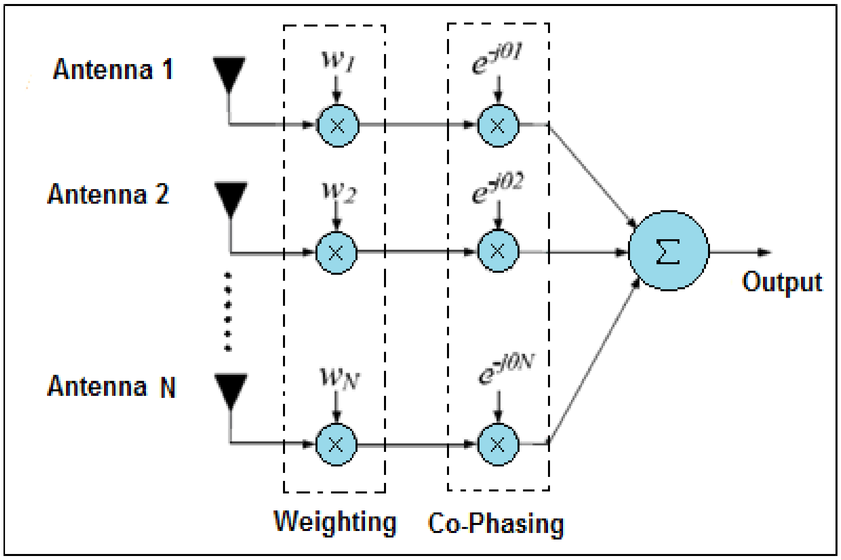

Figure 3.8. Block diagram of maximum ratio combining.

Among the four combining schemes the performance of MRC is the best but the most complicated. The performance of SC is the worst performance, but the equipment is simple to build, which is important to utilize in mobile phone. Since the dimension of the mobile phone become smaller. Additionally, since the computation complexity will be increased using MRC but not much more diversity gain would be obtained; SC is usually chosen as the diversity scheme [50].

3.6 Multiple Antenna Performance Metrics

To evaluate the performance of diversity and MIMO antenna systems, envelope correlation coefficient, and diversity gain are considered. In this section we will focus on the main performance features of the multiple antenna system and how to calculate these metrics.

3.6.1 Correlation Coefficient

For the diversity combining method to be efficient, two different versions of the same signal have to be achieved, otherwise the received signals are considered to be correlated. The correlation coefficient of the received signals can be characterized by the complex correlation coefficient and the envelope correlation coefficient. The complex correlation (ρ_c) is described as "the complex correlation between two signal envelopes" [51]. The magnitude and phase are used to compute correlation. The complex correlation coefficient between the signals at the mth and nth ports can be calculated as follows [30]:

$$\rho_c = \frac{\int_0^{2\pi}\int_0^{\pi} A_{12}(\theta,\phi)\, sin\,\theta d\theta d\phi}{\sqrt{\int_0^{2\pi}\int_0^{\pi} A_{11}(\theta,\phi)\, sin\,\theta d\theta d\emptyset \int_0^{2\pi}\int_0^{\pi} A_{22}(\theta,\phi)\, sin\,\theta d\theta d\phi}} \quad (3.4)$$

$$A_{ij} = XPR.E_{\theta n}(\theta,\phi)E_{\theta m}^{*}(\theta,\phi)P_{\theta}(\theta,\phi) + E_{\phi n}(\theta,\phi)E_{\phi m}^{*}(\theta,\phi)P_{\phi}(\theta,\phi) \quad (3.5)$$

where $E_\theta(\theta, \phi)$ and $E_\phi(\theta, \phi)$ denote the θ and ϕ components of the embedded element pattern of an antenna element, $P_\theta(\theta, \phi)$ and $P_\phi(\theta, \phi)$ are the angular density functions of the vertical and horizontal plane respectively, θ is elevation angle, ϕ is azimuth angle and the superscript (*) stands for conjugate transpose. XPR is the ratio of the averaged vertical power (P_V) to time average horizontal power (P_H) in the fading environment in linear form and is given by [52]:

$$\mathrm{XPR} = \frac{P_V}{P_H} \quad (3.6)$$

The other type of correlation metric is the envelope correlation (ρ_e), which is the correlation between two signal envelopes without considering the phase. ρ_e is always real as the phase is not defined. It is assumed that with independent Gaussian sources the envelope correlation is related to complex correlation in a Rayleigh fading environment as follows [53]:

$$\rho_e \approx |\rho_c|^2 \quad (3.7)$$

Another approach to compute the envelope correlation coefficient from the S-parameter characteristic of the antenna system has been derived. It shows that in some simple case of environment, such as uniform random field case, the correlation coefficient can be calculated from S- parameters. The envelope correlation coefficient in terms of the S-parameter of the antenna system can be expressed as [54]:

$$\rho_e = \frac{\left|S_{ii}{}^{*}S_{ij} + S_{ji}{}^{*}S_{jj}\right|^2}{\left[1-\left(|S_{ii}|^2+\left|S_{ji}\right|^2\right)\right]\left[1-\left(\left|S_{jj}\right|^2+\left|S_{ij}\right|^2\right)\right]} \tag{3.8}$$

where S_{ij} is the scattering parameter reflection coefficient for the input signal reflecting from port "*j*" into port "*i*", S_{ii} refers to the signal reflected at Port "*i*" from the signal incident at the same port. This method is more convenient way to calculate ρ_e since it is much easier to obtain the scattering parameters than the radiation pattern. The ρ_e ranges between 0 (no correlation) and 1 (full correlation).

3.6.2 Embedded Radiation Efficiency

Figure 3.9 illustrates a Multi-port antenna system consisting of N ports. For multiport antenna structure, efficiency per antenna element is of awareness which is known as embedded element efficiency. Embedded efficiency is calculated for element i when the antenna is excited at port and all other ports are terminated with 50 ohm load.

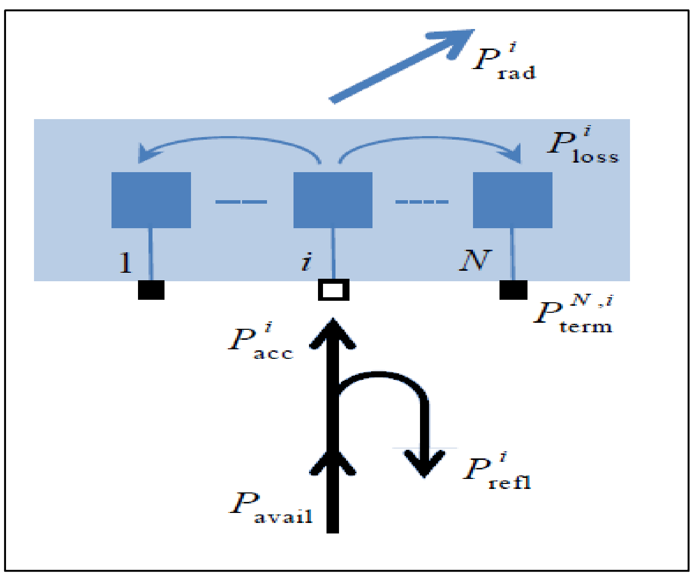

Figure 3.9. Embedded efficiency of multiport antenna [55].

There are two types of radiation efficiency: embedded element radiation efficiency e^i_{emb} which is defined as the ratio of the radiated power to the power delivered to the antenna and total radiation efficiency e^i_{tot} which is defined as the ratio of the radiated power to the maximum available power from the source, and can be defined as [55]:

$$e^{i}_{emb} = \frac{p^{i}_{rad}}{p^{i}_{acc}} = \frac{p^{i}_{rad}}{p^{i}_{avail}\,(1-\sum_{j=1}^{N}\left|S_{ji}\right|^{2})} \tag{3.9}$$

$$e^{i}_{tot} = \frac{p^{i}_{rad}}{p^{i}_{avail}} = e^{i}_{emb} \cdot e^{i}_{ref} \tag{3.10}$$

$$e^{i}_{ref} = 1-\left|S_{ii}\right|^{2} \tag{3.11}$$

where e^{i}_{emb} is embedded element for antenna element *i,* e^{i}_{tot} is the total embedded element efficiency for antenna element, e^{i}_{ref} is the reflection efficiency for antenna element i , P^{i}_{avail} is the power available from a matched source, P^{i}_{acc} is the power accepted by antenna when excited at port and P^{i}_{rad} is the radiated power when antenna is excited at port *i.* The total embedded radiation efficiency can be expressed much simple for a lossless structure by using scattering parameters, it can be defined as [55]:

$$e^{i}_{tot} = 1-\sum_{j=1}^{N}\left|S_{ji}\right|^{2} \tag{3.12}$$

and embedded radiation efficiency is:

$$e^{i}_{emb} = \frac{1-\sum_{j=1}^{N}\left|S_{ji}\right|^{2}}{1-\left|S_{ii}\right|^{2}} \tag{3.13}$$

3.6.3 Diversity Gain

Diversity gain (DG) is used to evaluate the diversity performance, DG is defined as the enhancement in the SNR achieved by combining the received signals relative to the SNR from a single antenna element in the same environment. DG can be calculated as the difference between a combined cumulative distribution function (CDF) relative to a reference CDF at a certain level of CDF. This level of CDF is typically considered to be 1%. The choice of the reference antenna results in different DG. There are two types of diversity gain depending on different references of CDF: apparent diversity gain and effective diversity gain. The apparent diversity gain (ADG) is the difference between the CDF of the combined signal and the one at the port with the strongest average signal levels in the same environment. Figure 3.10 [57] shows a graph of CDF of measured received signals as a function of SNR for ideal reference antenna and diversity antenna consisting of two parallel dipoles [56].

Instead of reading the ADG from the CDF-curves it can be obtained from the correlation coefficient. It is shown that calculating the ADG from equation (3.12) is much more accurate. For a two-port antenna, using selection combining scheme at 1% CDF level, the ADG can be computed as [58]:

$$\mathrm{ADG} = 10\sqrt{1-0.99\ |\rho_e|^2} \tag{3.14}$$

where 10 is the maximum apparent diversity gain at the 1% probability level with selection combining. Effective diversity gain (EDG) is defined as the difference between CDF of diversity-combined signal and the CDF of the signal at the port of an ideal single antenna at 1% CDF level (corresponding to radiation efficiency of 100%) measured in the same environment, EDG can be expressed as:

$$\mathrm{EDG} = \eta \mathrm{ADG} \tag{3.15}$$

Where η is the efficiency of the strongest antenna branch.

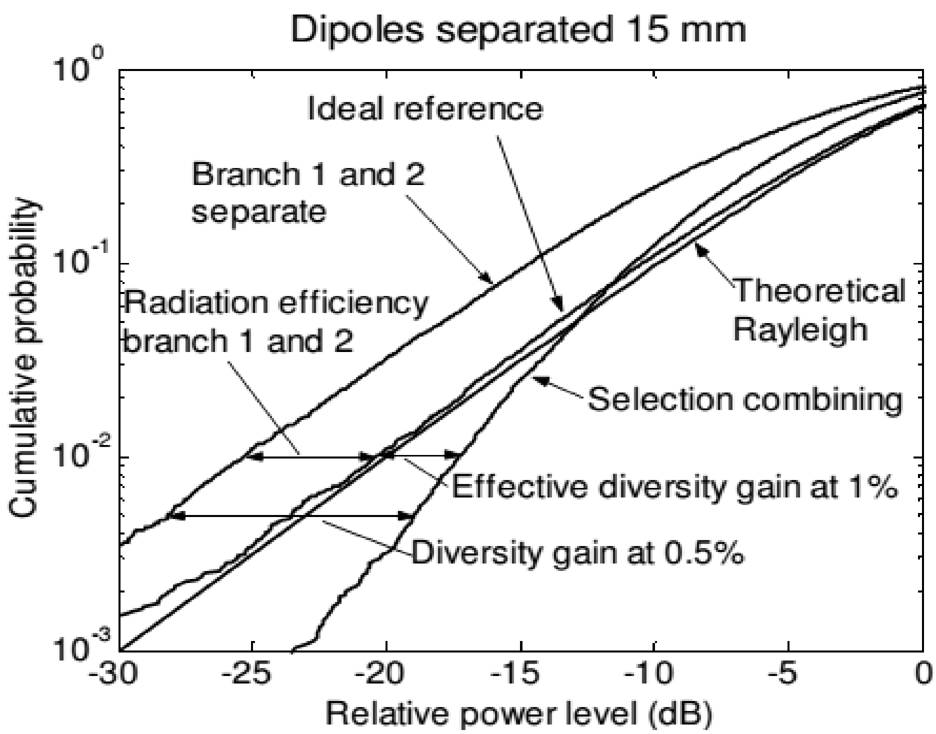

Figure 3.10. CDF of measured transmission function for ideal reference antenna and diversity antenna consisting of two parallel dipoles.

3.7 Summary

An introduction to multiple antenna system has discussed in this chapter. The two methods of exploiting the MIMO channels: spatial multiplexing and space-time coding have also been presented. The four typical diversity combining methods: switched combining, selection combining, equal gain combining and maximum ratio combining are discussed. Also antenna diversity spatial, pattern and polarization techniques have summarized. Three relevant metrics and their calculations for diversity performance have described: envelope correlation coefficient, embedded efficiency and diversity gain.

4

Single Folded Loop Antenna Design

4.1 Introduction

In this chapter a design of a single element folded loop antenna (FLA) is discussed and the simulation results of the proposed FLA antenna are presented. After that parametric analysis are also shown, which is helpful to achieve best results. Antenna performance parameters such as return loss, input impedance, peak realized gain, 2D/ 3D radiation patterns and current distributions are examined.

4.2 Antenna Geometry

The antenna have been designed for a typical hand held device such as Smartphone. While designing the antenna the form factor of a practical Smartphone of 110mm x 50mm was considered. The overall geometry of the proposed antenna is illustrated in Figures 4.1 (a-c). The antenna consists of a closed loop metal structure folded pattern mounted on an L-shape dielectric carrier which is placed at the top of printed circuit board (PCB) board as shown in Figure 4.1(a). The board have a thickness of 0.8mm and an area of 110 mm × 50 mm is made of FR4-Epoxy material with a relative permittivity of 4.4 and a loss tangent of 0.02. The carrier is made of material of relative permittivity of 3 and a height of (h=5mm) from ground plane, A 50Ω lumped port is used to excite the loop antenna pattern on the front side of the main board connected to the feeding point of the loop, while the other end is connected to the ground plane at the shorting The dimensions of the folded loop antenna and the ground plane in an unfolded form are detailed in Figure 4.1 (c). The folded loop antenna track has a width of 1 mm in most parts except that the section (L1) and section (L2) are 2 mm width. The total length of the folded and meandered loop strip from A to B is about 117 mm (about 0.25λ at 2.5GHz). The detailed optimized dimensions of the proposed folded loop antenna metal pattern model are given in table 4.1.

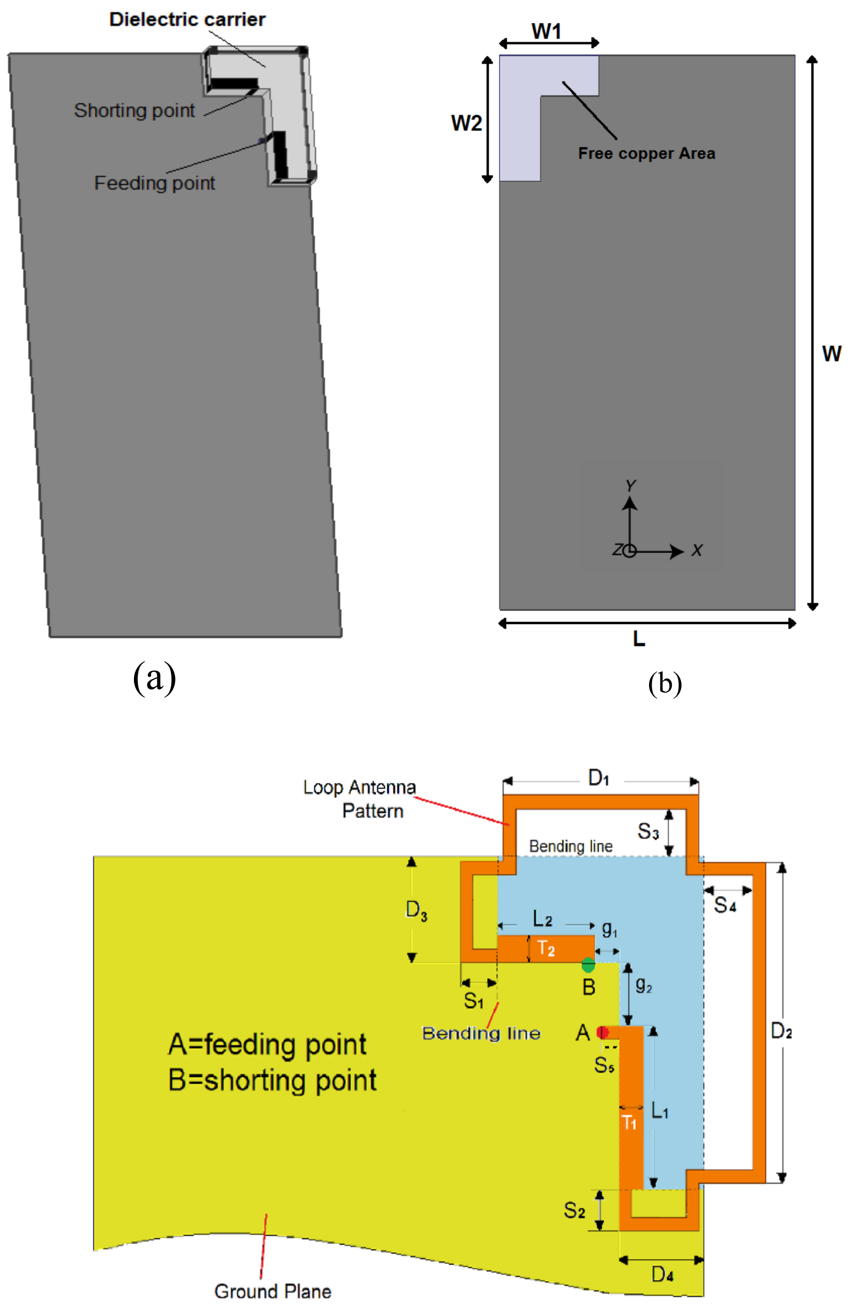

(c)

Figure 4.1. Antenna geometry of the proposed FLA antenna (a) Top layer (b) Bottom layer (c) Detailed dimensions of the antenna unfolded into a planar structure.

Table 4.1. Detailed dimensions of the proposed antenna

Unites :mm									
D1	D2	D3	D4	L1	L2	S1	S2	S3	S4
16	24	8	7	9	8	3	3	3.5	4
S5	T1	T2	g_1	g_2	L	W	W1	W2	h
2	2	2	2	8	110	50	17	25	5

4.3 Parametric Analysis

The antenna's performance is changing depending on many parameters, in our study three of the parameters are examined: the length of lower stripe (L1), the length of upper stripe (L2), and the carrier dielectric material (dielectric constant ε_r). In this subsection, the impact of varying antenna parameters on its performance and frequency response are investigated. All parametric study results are presented and considered with varying one parameter at a time and the other parameters are fixed to a certain value, whereas the best value obtained from the individual parametric study results. The antenna component values and the antenna structure were first modeled with variables. Then, HFSS has been set to run simulations for number of different values of the variables. The main purpose is to find a better performance of the folded loop antenna to cover the required band.

4.3.1 The Effect of Length of lower stripe L1

Figure 4.2 shows the effect of changing the length (L1) on the antenna S-Parameters (S11) performance. Four values 8, 9, 10 and 11mm of length of L1 have been chosen to monitor the changes in the antenna performance, other values are set to a certain values. It's noticed that as the length of (L1) stripe increases the resonant frequencies will shift to the left in the graph, which mean that the resonant frequency of the antenna will decrease. L1 variation have the effect on the high resonances frequency bandwidth more than the value of return loss.

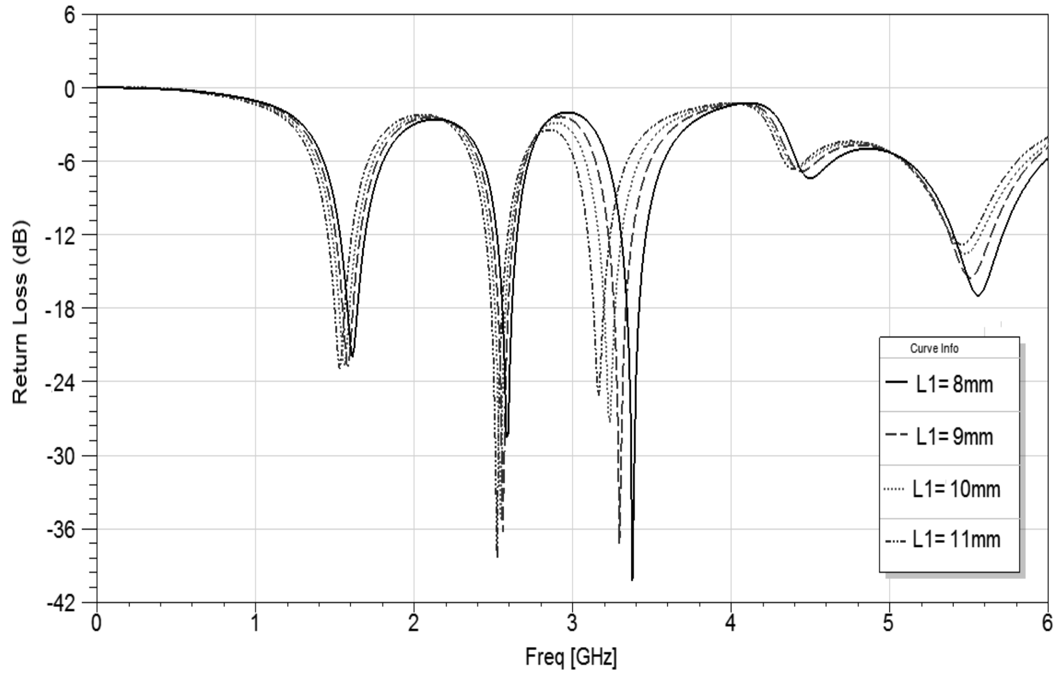

Figure 4.2. Simulated results as a function of length L1 (Lower stripe length).

4.3.2 Effects of the Upper Stripe Length L2

The variation in L2 also affects the antenna resonances. Figure 4.3 shows that as the length of the L2 increases the S-Parameter S11 curve shift to the left . L2 has the effect on antenna return loss values and bandwidth less than the effect of L1.

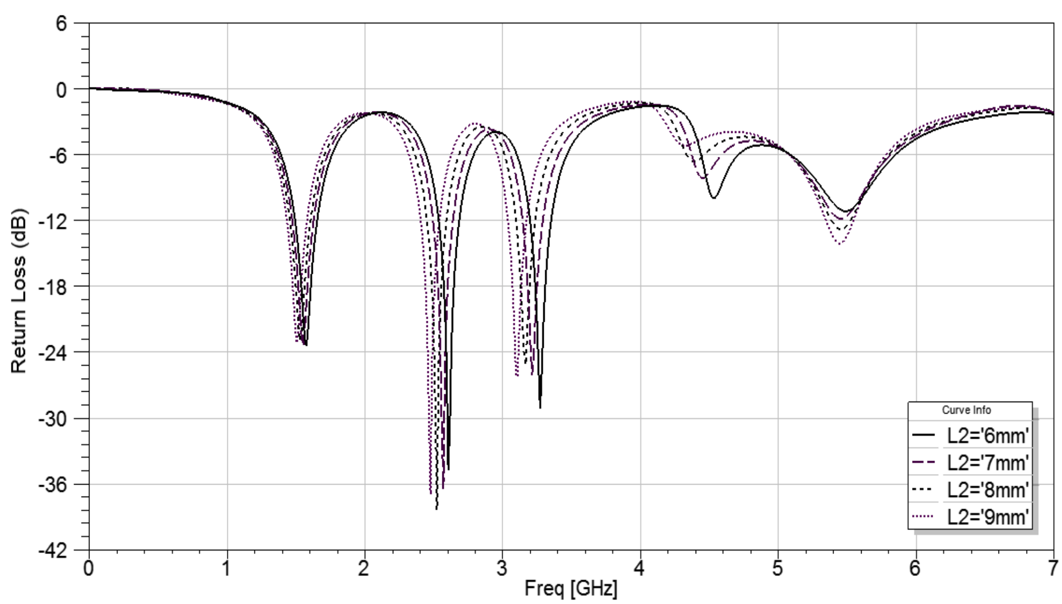

Figure 4.3. Simulated results as a function of length L2 (Upper stripe length).

4.3.3 The Effect of Dielectric Loading

Antennas can be loaded by a dielectric material, the shape and permittivity of the material determines the effective wavelength. As the wavelength is shorter in a high permittivity material, the effective wavelength of an electromagnetic wave is less than that in free space. This is due to the concentration of the electric field in high permittivity materials. Therefore, the antenna size can be reduced and hence the folded loop antenna can be made smaller in size. Apart from size reduction, another reason to use dielectric material is more resistant to detuning when placed to other objects like the human body in the case of the handset antennas. If the dielectric material is used in the antenna with the electric fields or currents are high, it makes the antenna more efficient than its all metal counterpart .The impact of the dielectric loading on the antenna resonance have been evaluated using HFSS. Four values of relative permittivity (ε_r) ranging from 2 to 5 with 1 steps were used to investigate the change in the antenna return loss. As shown in Figure 4.4, the variations in ε_r have a significant impact on the antenna operating band. We observe that as we increase the relative permittivity of the dielectric material the resonance frequency will shift to left and the return loss magnitude will increase. The simulated antenna return loss with and without a dielectric slab are given in Figure 4.5.

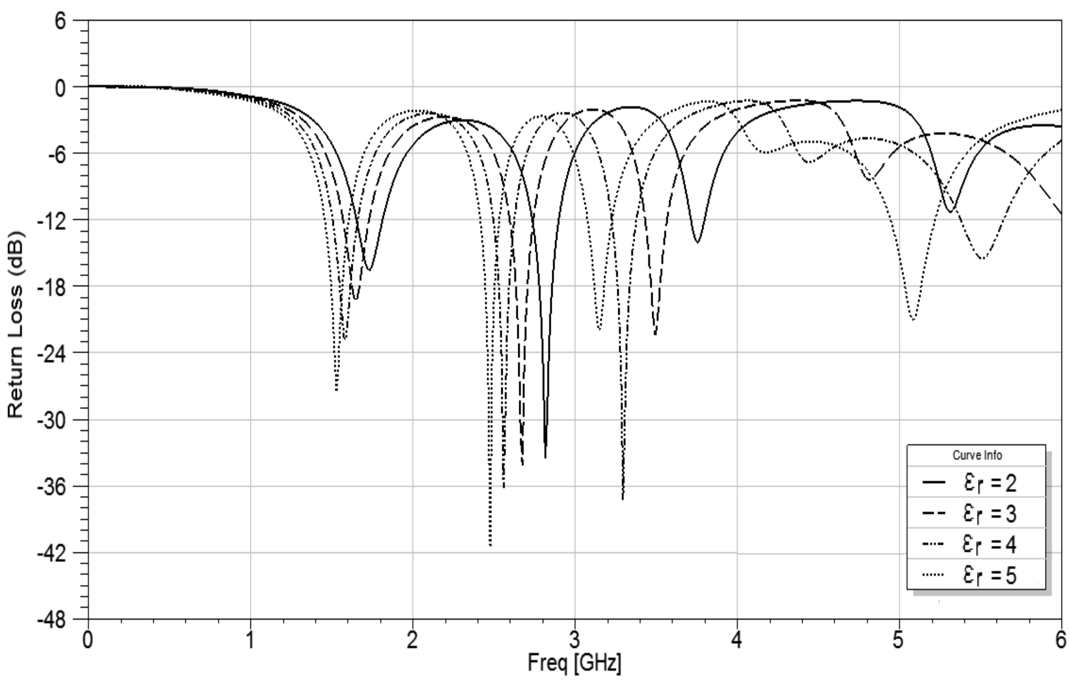

Figure 4.4. Simulated results as a function of dielectric relative permittivity

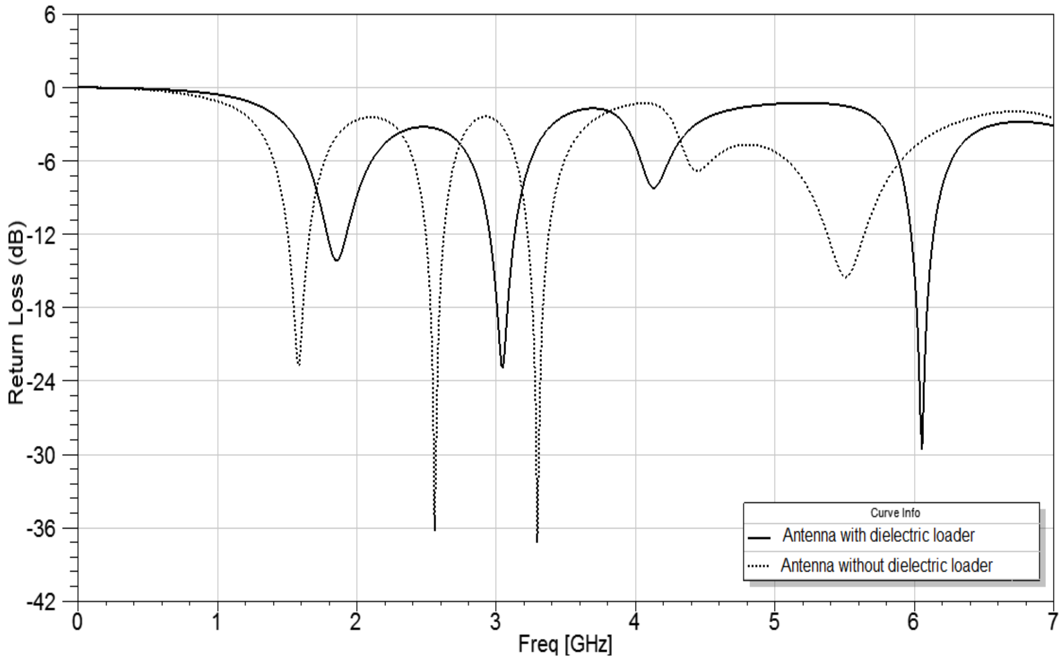

Figure 4.5. Simulated S-parameter characteristics with and without a dielectric slab.

4.4 Simulation Results

In this subsection the simulation results of the optimized single element folded loop antenna are shown below.

4.4.1 Return Loss

Figure 4.6 illustrates the simulated impedance bandwidth of the optimized proposed loop antenna. The graph shows the return loss as a function of frequency *f* which sweeps from 1 GHz to7 GHz, as seen. Five impedance bandwidths for the proposed antenna have been determined, the bandwidth for these bands has been determined according to the reflection coefficient (S11) level of -6dB. These bands are marked as band no.1 (1.4 GHz – 1.77 GHz), band no.2 (2.4 GHz – 2.7 GHz), band no.3 (3.14 GHz – 3.5 GHz), band no.4 (4.3 GHz – 4.53 GHz) and band no.5 (5.1 GHz – 5.9 GHz). It noticed that as the frequency increases, the operating frequency modes have wider bandwidth. In band 1, the best S11 is of -21dB, band 2 at -30 dB, band 3 at -31 dB, band 4 at -8 dB, and band 5 at -16dB.

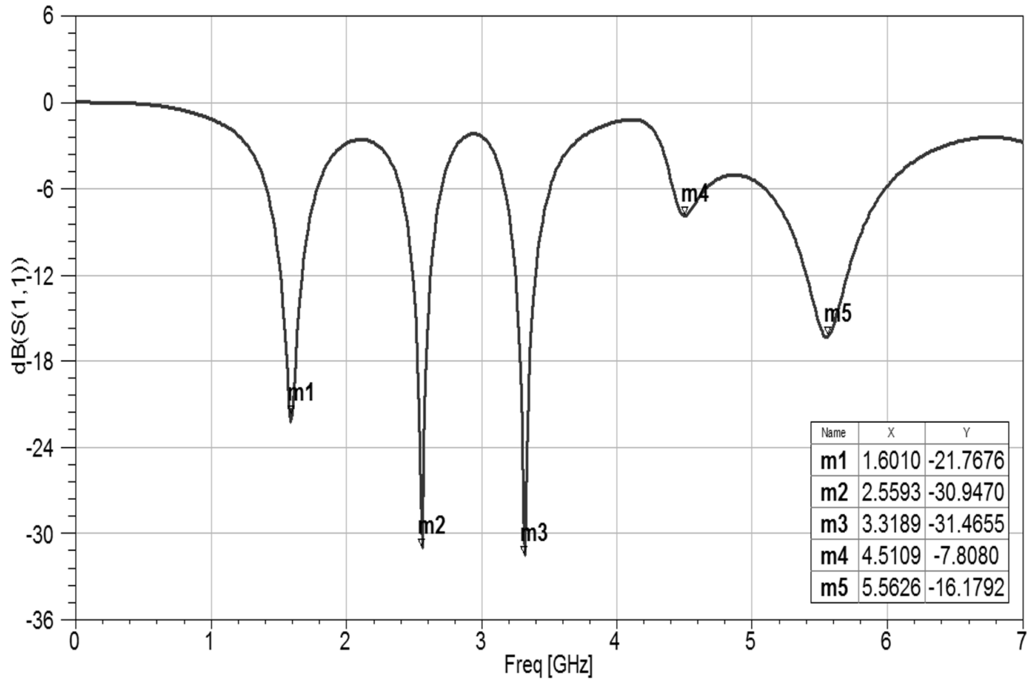

Figure 4.6. Simulated return loss of single FLA.

The simulated real and imaginary antenna input impedance plot is shown in Figure 4.7. In general the impedance matching plots agree well with the required impedance matching.

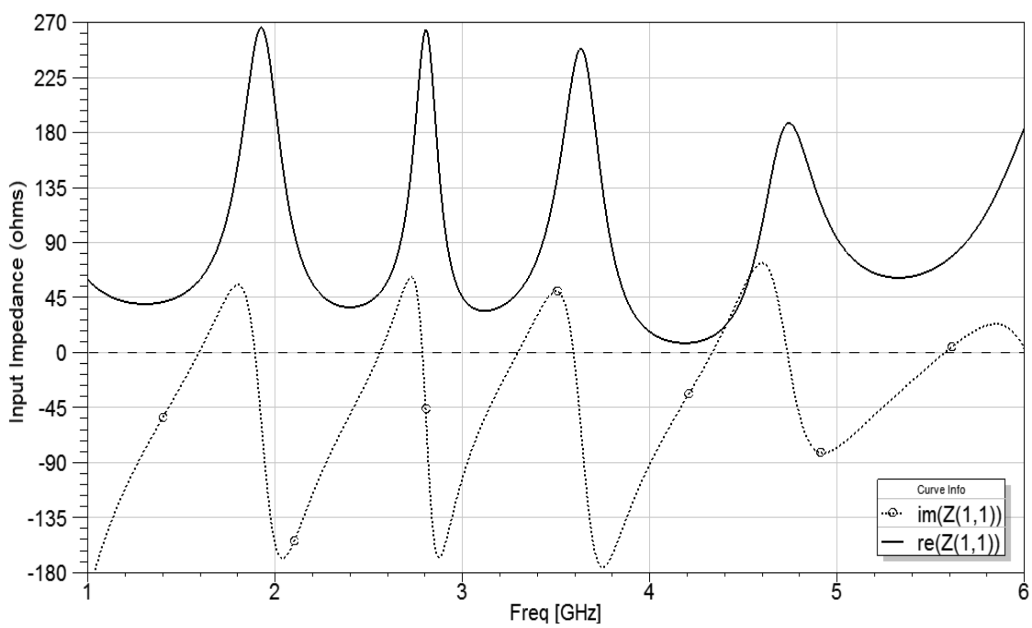

Figure 4.7. Real and imaginary parts of input impedance of proposed antenna.

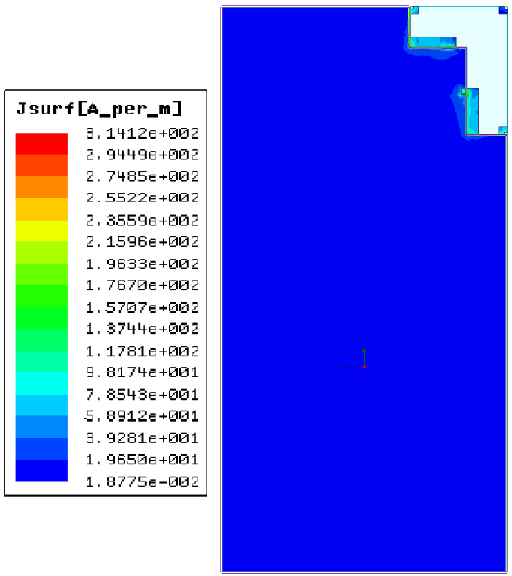

(a) 1.6 GHz

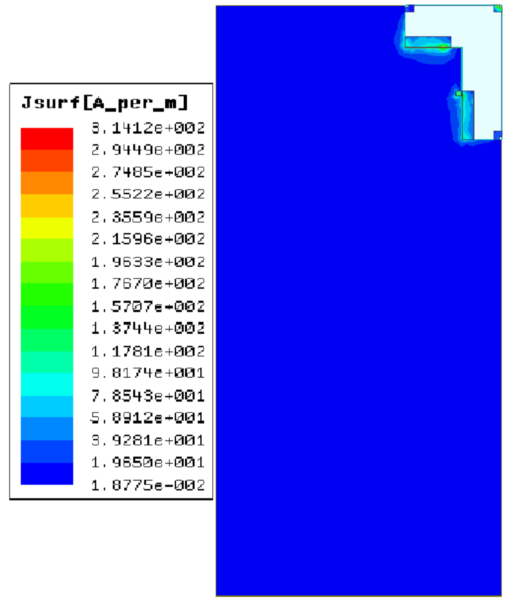

(b) 2.55 GHz

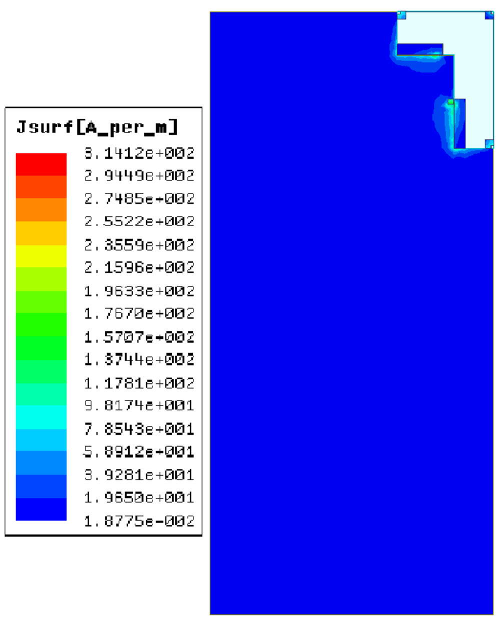

(c) 3.3 GHz

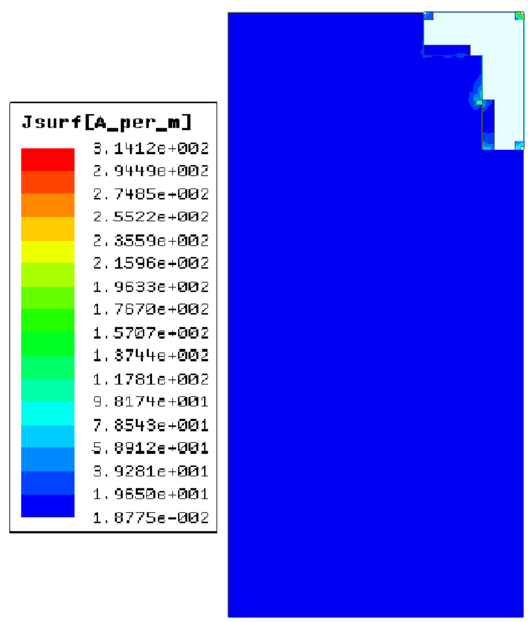

(d) 5.5 GHz

Figure 4.8. Simulated surface current distributions at center resonant frequencies of the four resonant modes for the proposed antenna with the system ground plane at (a) 1.6 GHz, (b) 2.55 GHz, (c) 3.3 GHz, and (d) 5.5 GHz.

4.4.2 Current Distribution

The current distribution is plotted in Figures. 4.8 (a-d), the strongest current distribution is on the meandered line and it is seen that the induced current in the ground plane is negligible except very close to the antenna which prove the advantage of this balanced loop antenna.

4.4.3 Radiation Pattern

Figures 4.10 (a-d) show the simulated 2D co-polarization and cross-polarization realized gain radiation patterns for the XZ and the YZ planes for 1.6 GHz, 2.55 GHz, 3.3 GHz and 5.5 GHz. The related 3D radiation patterns are also shown in Figures 4.9 (a-d), the radiation patterns are close to Omni-directional radiation pattern, and these features are suitable characteristics for mobile phones. Figure 4.9 shows the peak gains, the simulated antenna gain over the band varied from around 0.2 - 3.0 dBi, so better communication quality for LTE/WLAN/WiMAX systems can be realized as well.

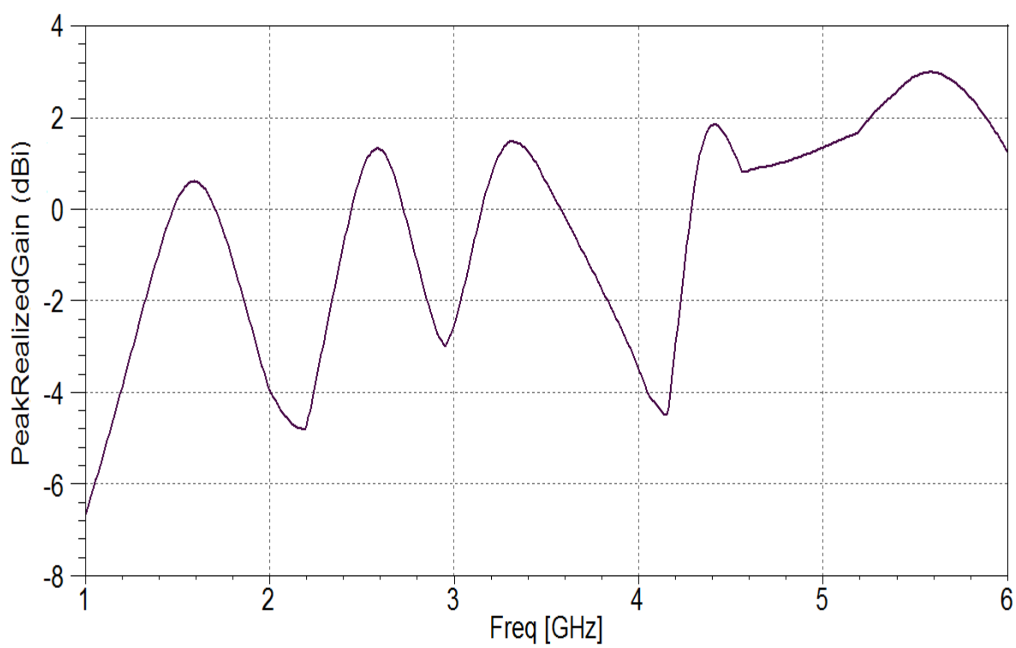

Figure 4.9. Simulated peak realized gain of the loop antenna.

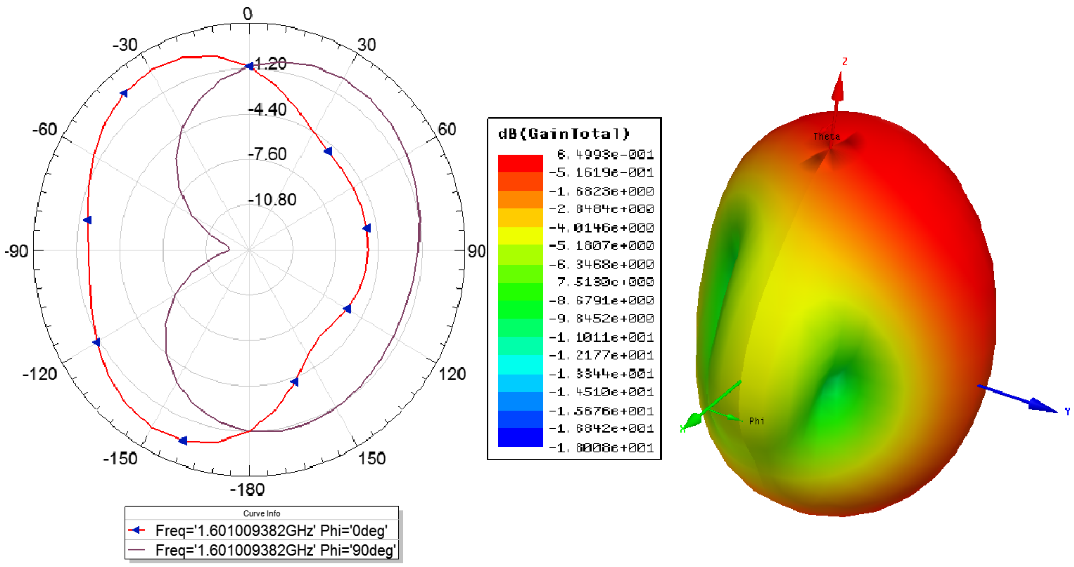

(a) 1.6 GHz

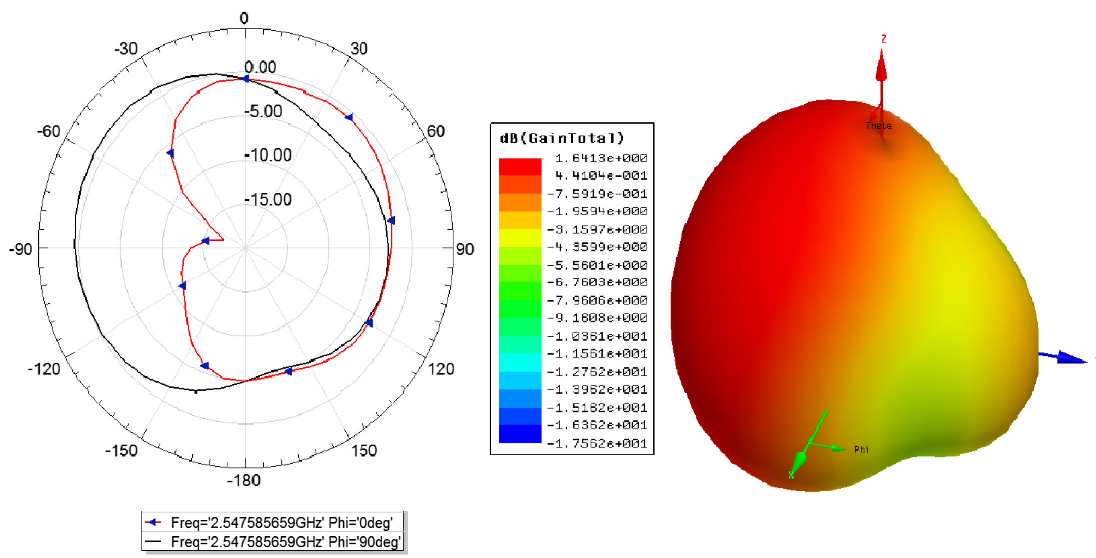

(b) 2.55 GHz

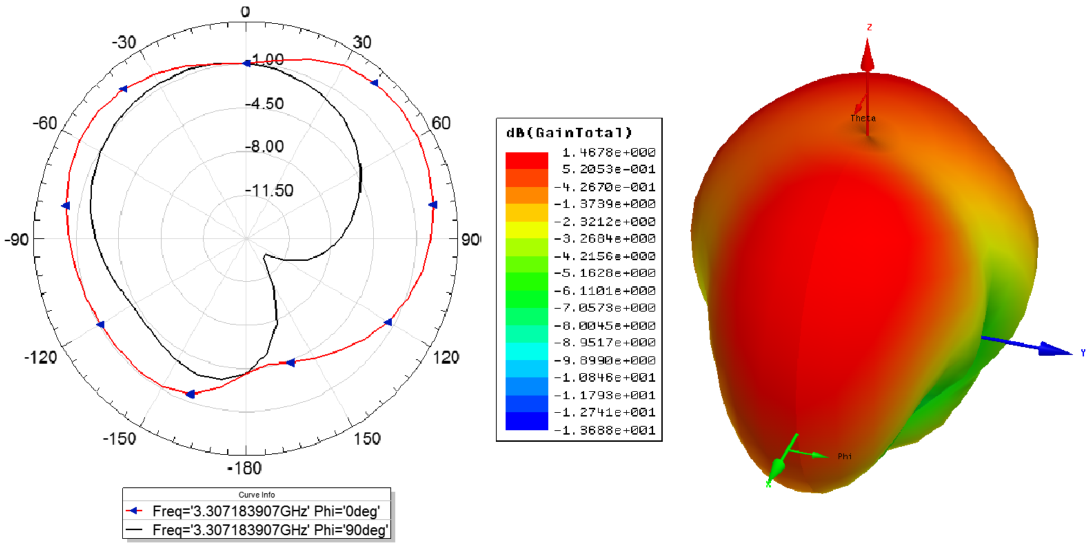

(c) 3.3 GHz

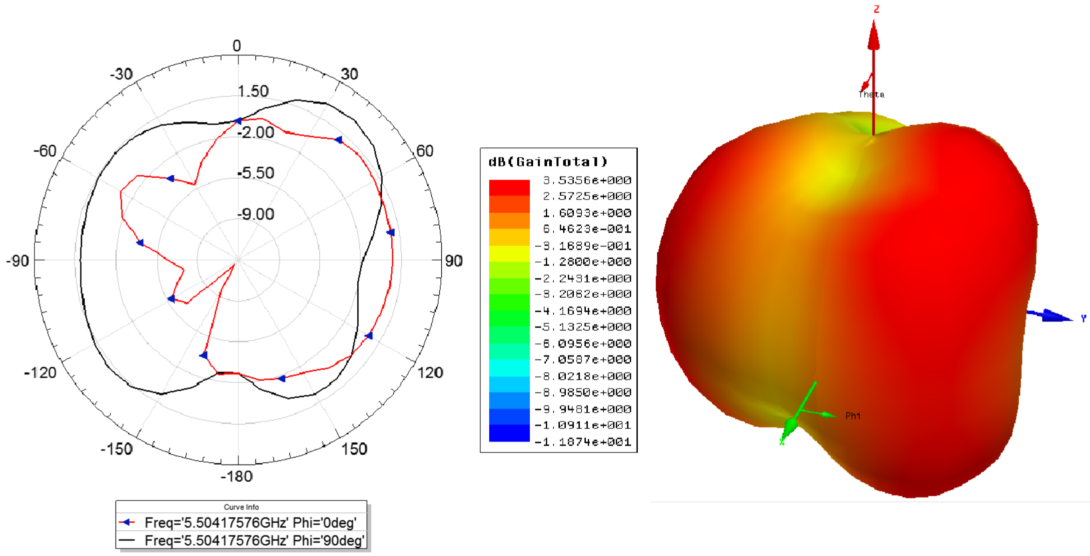

(d) 5.5 GHz

Figure 4.10. Simulated radiation pattern of single element antenna at (a) 1.6 GHz, (b) 2.5 GHz, (c) 3.3 GHz, and (d) 5.5GHz.

4.5 Summary

In this chapter a multiband single folded loop antenna designed for mobile phones has been demonstrated and studied, the proposed loop antenna generates four impedance bandwidths (1400-1770, 2400-2700, 3146-3500, and 5090-5900 MHz) which can be used to cover the multiple LTE/WLAN/WiMAX mobile phone operations. The antenna structure is simple, compact and flexible and it makes the design easy to manufacture. The results of the numerical software simulation are in good agreement as expected where the radiation pattern have semi-omnidirectional antenna features and have a good gain.

5

MIMO Design Simulation

5.1 Introduction

In this chapter, a design of two element MIMO folded loop antenna on smartphone will be deployed with different configuration of the multiple antenna based on the antennas locations and orientations on the PCB. The comparisons between the different configurations depends on performance characteristics, isolation and correlation coefficients. Also antenna performance parameters such as return loss, peak realized gain, radiation patterns and current distributions will be examined.

5.2 Two Elements MIMO Antenna Design

To enhance the communication link performance such as data rate through the applying the MIMO system and to mitigate the multipath fading through the use of the diversity deployment scheme using multiple antenna scheme. Analytical studies have shown that to achieve a better isolation between the multiple antennas the separation between antenna elements has to be at least half wavelength [59], because the ground plane dimensions is small, this will make a challenge to have a good separation between the two antennas.

Three different antenna configurations characterized by different antenna locations and orientations on the PCB are designed and simulated to compare the results, investigate the influence on the MIMO performance, the aim of this study is to find the best results depending on many aspects such as return loss, mutual coupling and diversity gain.

5.2.1 Case 1

Figure 5.1 shows the geometry of the MIMO antenna orientation model for the first case, two similar FLAs are placed in the upper right and left corners of the ground plane in a symmetric configuration of the two antenna, the distance between the two antennas is 16mm (0.13 λ at 2.5 GHz). Figure 5.2 shows the simulated results of reflection coefficient and isolation of antenna configuration, both $S_{11}$and S_{22} are found to be same due to symmetry of the antennas. As the two antennas are close to each other, the minimum isolation between the two antennas is found to be 12 dB, the isolation at 2.5GHz is found to be 15dB.

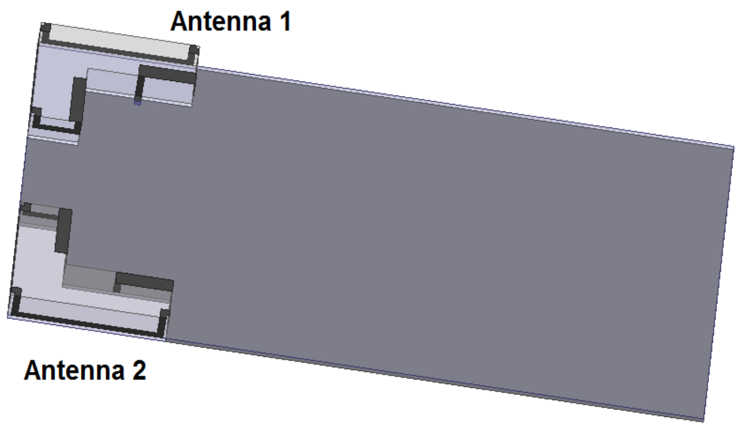

Figure 5.1. Geometry of multiple antenna orientation in case 1

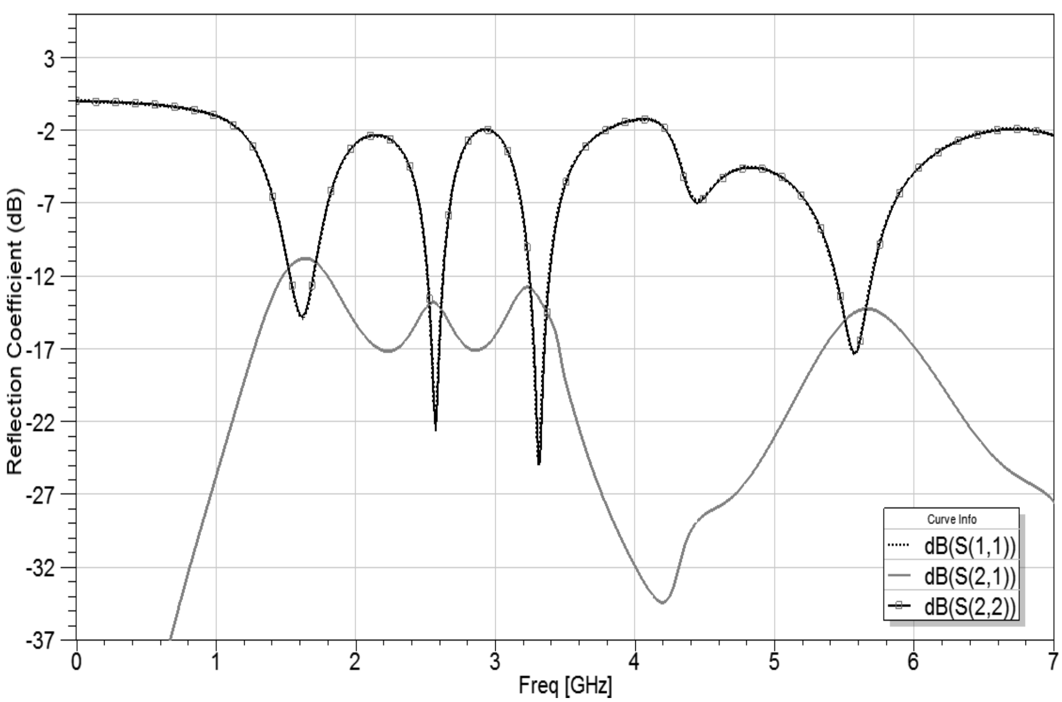

Figure 5.2. The reflection coefficient and isolation for the case 1

5.2.2 Case 2

The second antenna configuration geometry model is shown in figure 5.3, the two FLAs are placed in the two vertical corners of the ground plane (upper and lower) edge. In this configuration, the separation between the two antennas is increased from 0.13 λ to 60 mm (0.5 λ at 2.5 GHz). The reflection coefficient response and isolation of the two antennas is shown in the figure 5.4. It can be seen that the minimum isolation is increased to 22dB and the isolation band is improved to 32 dB at 2.5 GHz.

Figure 5.3. Geometry of multiple antenna orientation in case 2

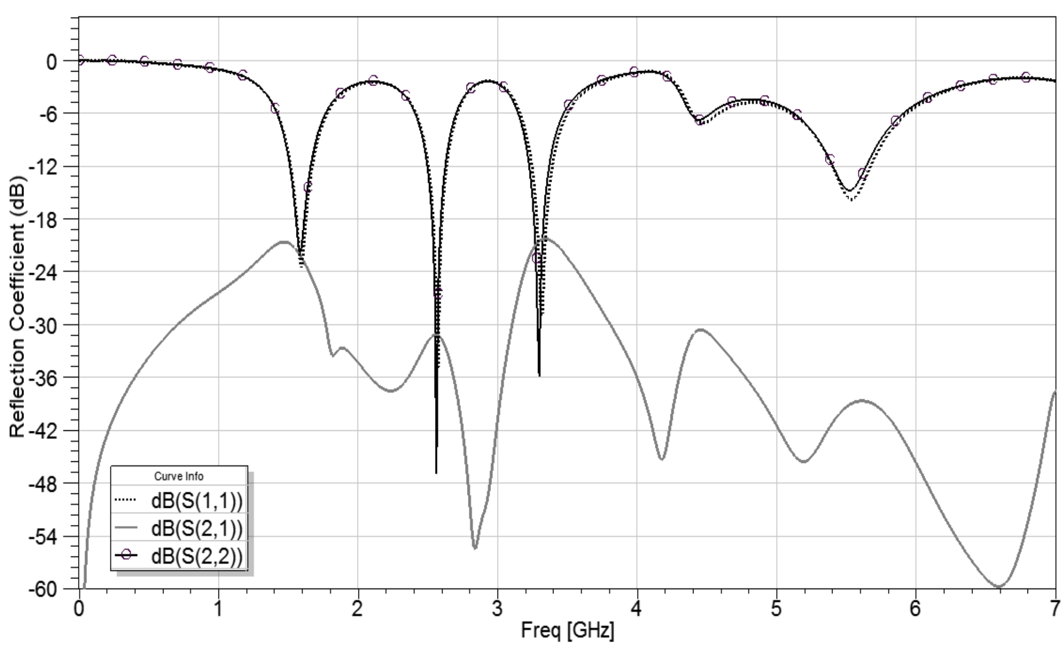

Figure 5.4. The reflection coefficient and isolation for the case 2

5.2.3 Case 3

The third configuration geometry model is shown in figure 5.5, the two FLAs are placed in the opposite direction of the ground plane corners where the two FLAs are located orthogonally, which leads to more isolation between the antennas, the distance between antennas the antennas is approximately 70mm which corresponds to 0.6λ at 2.5GHz. The simulated reflection coefficient and isolation performance results of the antennas are shown in figure 5.6. The minimum isolation between the antennas found to be the same as case no.2 where it found to be 22 dB and the isolation at 2.5 GHz band is increased to 35dB.

Figure 5.5. Geometry of multiple antenna orientation in case 3

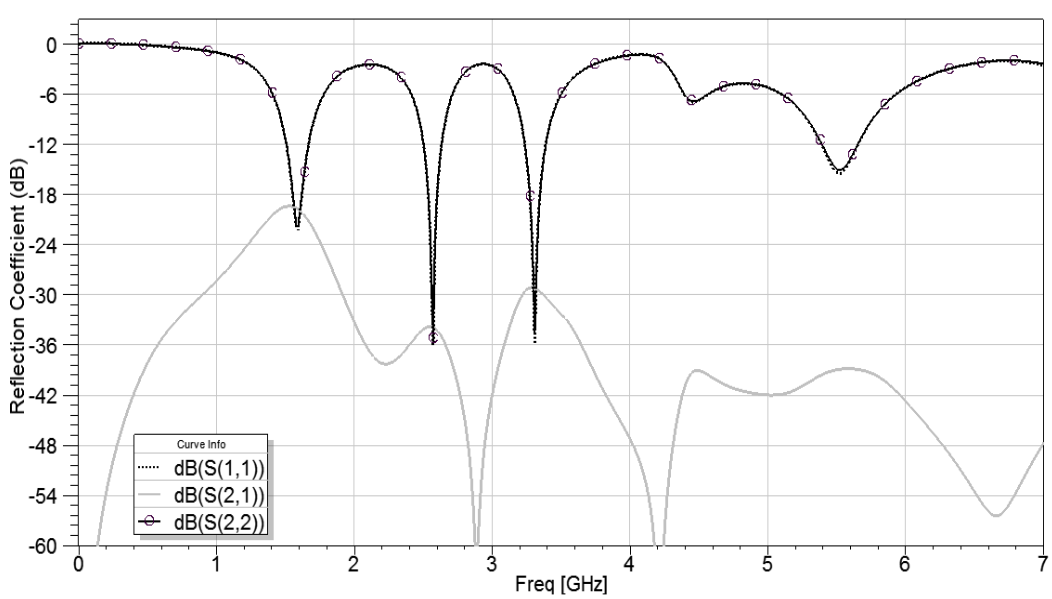

Figure 5.6. The reflection coefficient and isolation for the case 3

5.3 Comparison of the Various Orientations

MIMO performance strongly depends on antenna elements spacing and coupling. Three antenna configuration are studied to decide which cases is used according to three aspects: return loss results of the antennas, mutual coupling between the two antennas and correlation coefficient achieved by the configuration.

5.3.1 Return Loss Comparison

The performance difference between varies S-parameters of multiple antenna arrangements cases are examined, Figures 5.7 (a) , (b) show the different performance characteristic of the reflection coefficient (S_{11},S_{22}) of the multiple antenna system of for the three cases of the antenna configuration, It can be seen that the two FLAs of case no.1 have smaller different reflection coefficient compared with case no.2 and no.3, this is because the two antenna are closer to each other than the case no.1 and case no.2. Also, at case no. 2 the two FLAs placed in upper and lower corner of ground plane makes the distance between the two antennas is enough to get good performance compared with case no.1. Case no.3 has the largest return loss results and there is a small difference compared with case no. 2 due to the mutual coupling because of the orthogonality of the configuration.

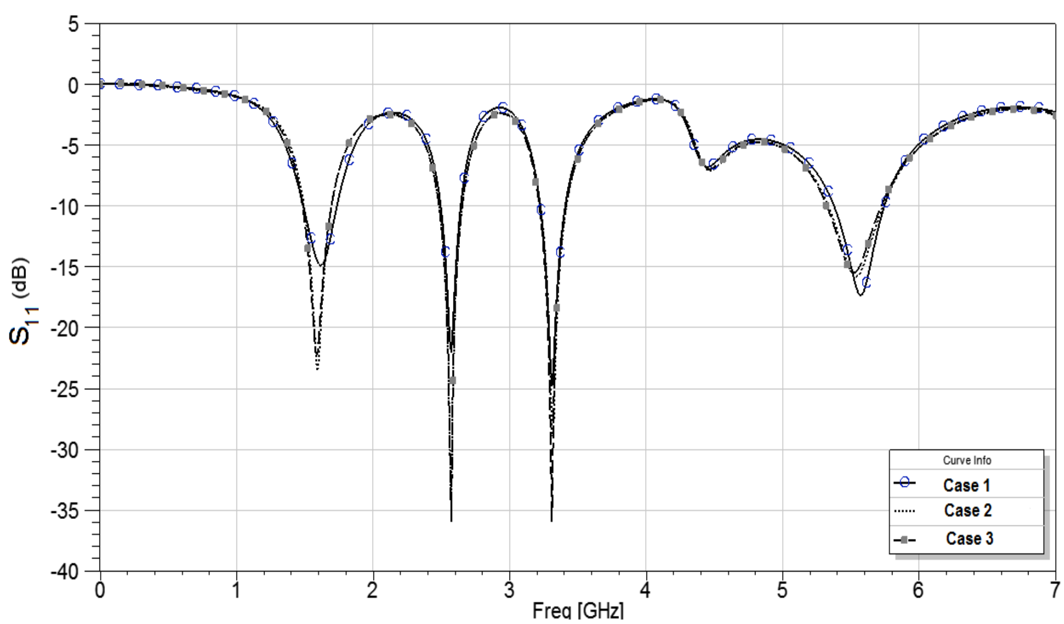

(a)

.

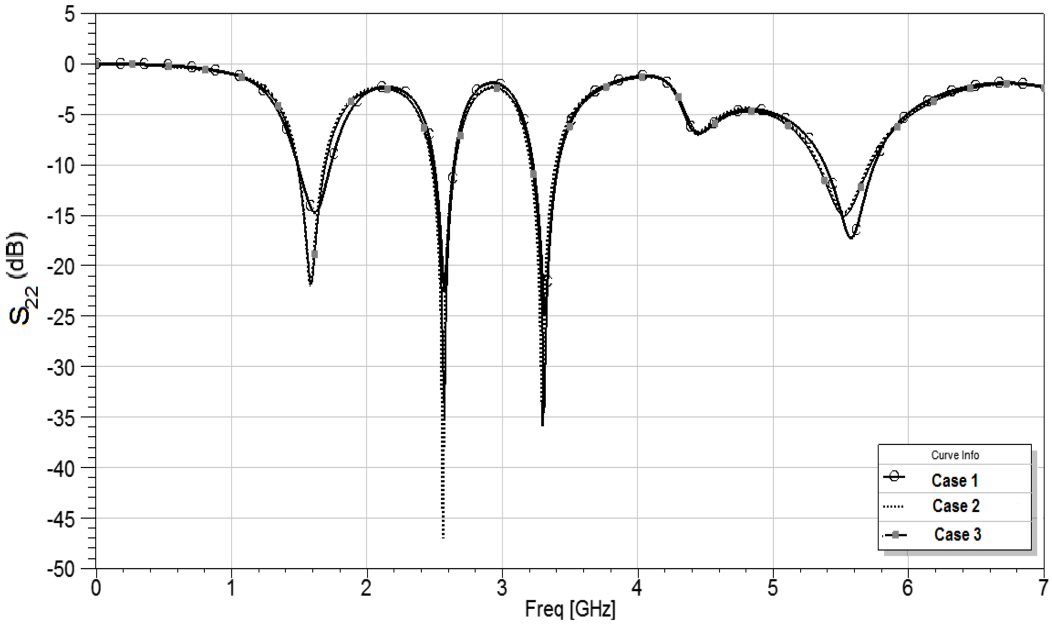

(b)

Figure 5.7. Comparison of (a) S11 and (b) S22 for different configuration of multiple antenna.

5.3.2 Mutual Coupling Comparison

Figure 5.8 shows the comparisons of the mutual coupling of the three cases of antenna placement on the ground plane to find the isolation performance of the dual-element FLA antennas. It can be seen clearly that case no.1 has the weakest isolation among the three cases because the antennas are close to each other, case no.2 comes in the second, and case no.3 has the strongest isolation performance in the most of the frequency band due to the larger separation compared to case 1 and the orthogonal orientation of the two antennas produce less current and field interaction between the antennas.

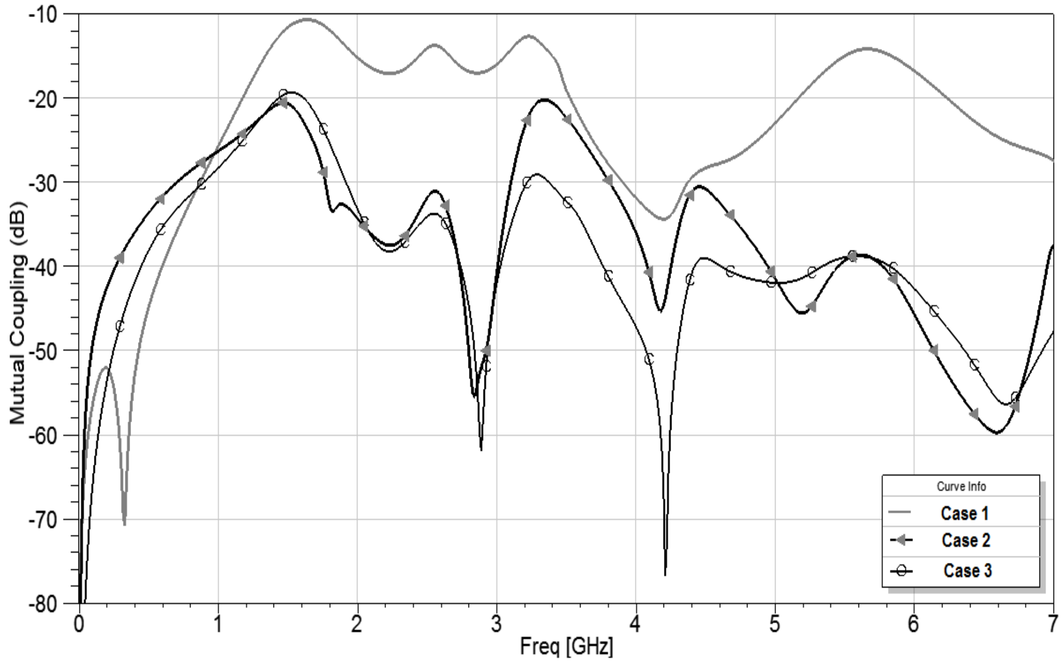

Figure 5.8. Plot of S21 (mutual coupling) for all configurations

5.3.3 Envelope Correlation Performance Comparison

Diversity performance is the serious importance of multiple antenna systems. Different antenna spatial orientations in the space will produce different diversity results, Figure 5.9 shows the comparison of envelope correlation coefficient (ECC) against frequency calculated using equation (3.8) between each of the three multiple antenna system configuration. As expected, case 3 gives the best correlation characteristics with a lower ECC value, while the difference with case 2 is negligible. Case no.1 has an average of higher envelope correlation compared to other cases due to close separation between the elements, but still satisfies the $\rho_e < 0.5$ criterion.

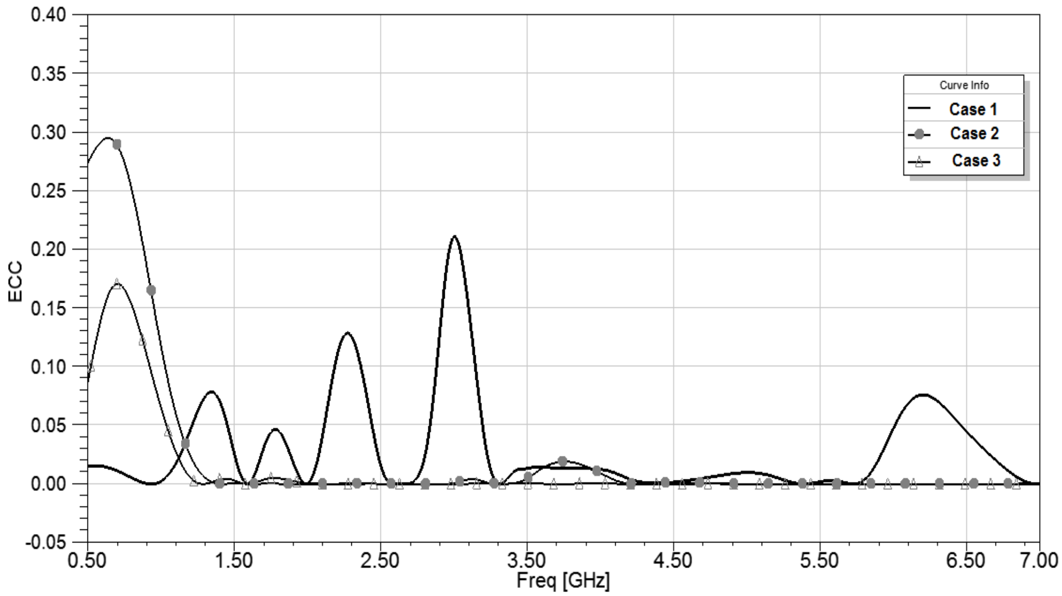

Figure 5.9. Envelope correlation coefficient for all configurations.

5.4 Simulated Reflection and Radiation Response Results

Between the three cases of MIMO antenna configuration, case 1 could avoid the antennas being covered by the user's hand as the performance of the antennas could be degraded if they are covered by the user's hand. Case one was chosen to further study the performance of each antenna. Antenna performance parameters such as reflection coefficient, peak realized gain, radiation patterns and current distributions are presented. Also diversity performance is evaluated.

5.4.1 Return Loss

The simulated return loss performances of each antenna of the MIMO configuration are shown in Figure 5.10. The S11 is the same as the single antenna design. The reflection coefficients performance of the four resonant bands is less (about 4dB) than the performance of the single antenna simulation design results this is because the two antennas are close to each other which results in the degradation of the performance of the two antenna.

There is a multiband response occurring at various groups of frequencies, the impedance bandwidths for these bands have been determined by the reflection coefficient of -6dB, these bands are marked as band no. 1 (1.39 GHz – 1.82 GHz), band no.2 (2.4 GHz – 2.7

GHz), band no. 3 (3.15GHz – 3.5 GHz), band no.4 (4.4GHz – 4.5 GHz) and band no.5 (5.15GHz -5.9GHz). In band 1, the greatest S11 value is -15 dB at 1.62 GHz, -22 dB at 2.57 GHz in band 2, -24dB at 3.3 GHz in band 3 , -7 dB at 4.47 GHz in band 4 and -17 dB at 5.58 GHz.

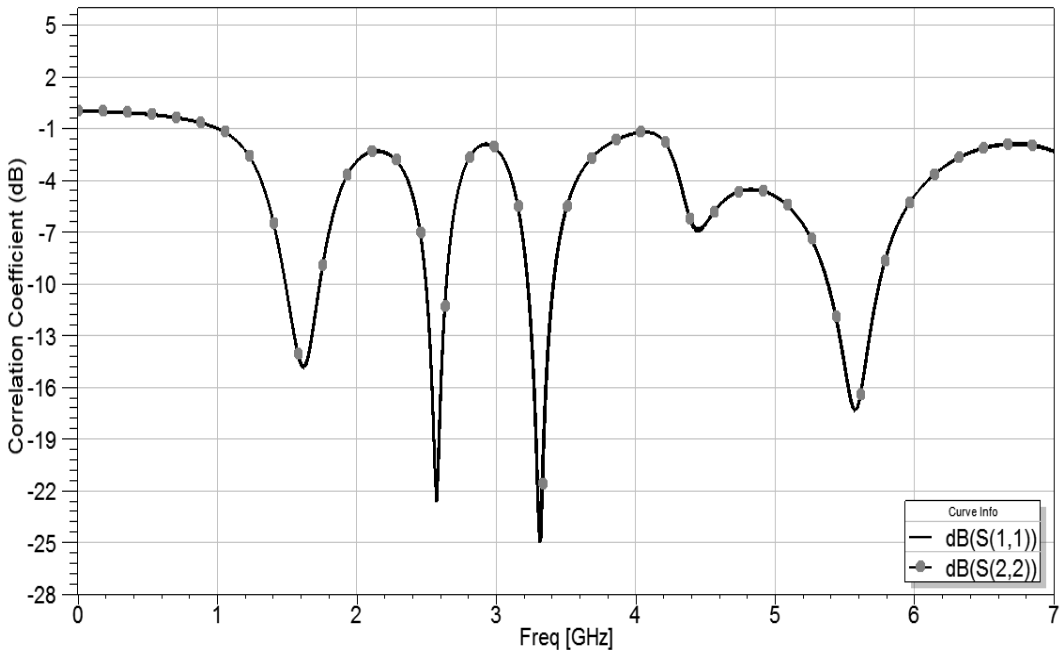

Figure 5.10. Simulated correlation coefficient (S_{11}, S_{22}) for case1.

5.4.2 Mutual Coupling Performance

Figure 5.11 shows the isolation performance between both antennas, as the two ports S12 and S21 are symmetrical, both graphs being exactly the same and plots are overlying on each other as one curve. Isolation performance of more than 10 dB between the ports of antennas has been achieved for all cases and much lower for different areas in the particular band, the mutual coupling in band 1, there is a maximum mutual coupling of -10.7dB at 1.61 GHz, band 2 of -13.8 dB at 2.57 GHz, band 3 of -12.7 dB at 3.23 GHz ,band 4 of -28 dB at 4.5 GHz and band 5 -14.2 at 5.6 GHz, as mutual coupling between the antenna couples is very low at resonance frequencies, therefore a low correlation between the antennas could be realized and would lead to good diversity gain.

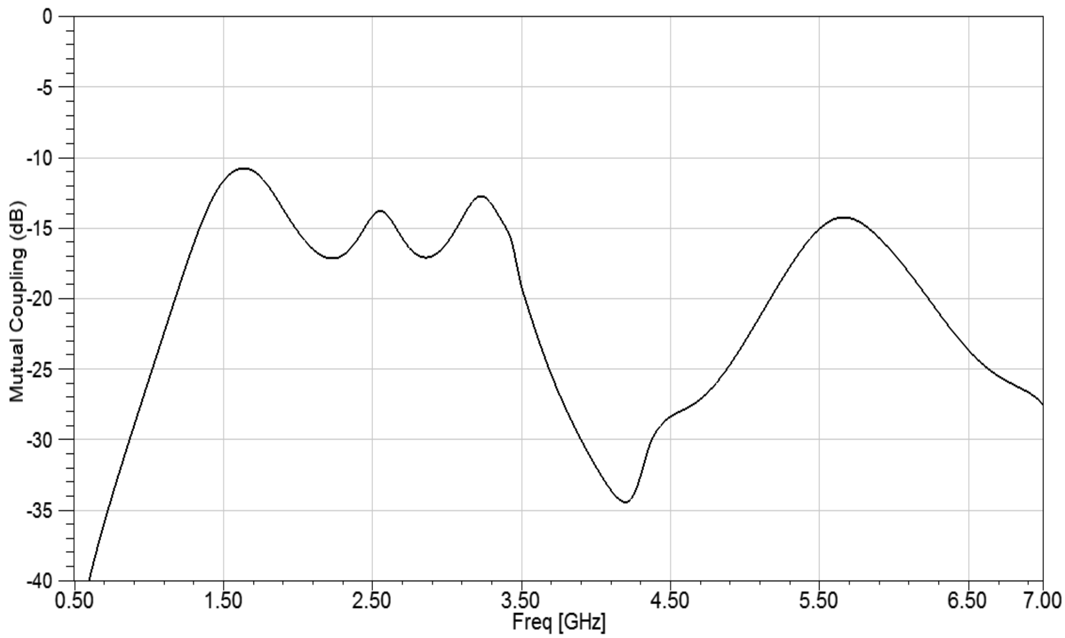

Figure 5.11. Variation of mutual coupling vs. frequency with a -6 dB criteria for a two element design for case1.

5.4.3 Antenna Gain Performance

The study for the peak realized gain was performed and the results are presented in Figure 5.12, where both of the antennas have a positive gain located in all segments of the five bands. For the first band, the impedance bandwidth using -6dB as the measures is in the range of 1.39 GHz to 1.82 GHz. This results in a total bandwidth of 430 MHz. In this band, there is a minimum gain of -0.24 dBi at 1.39 GHz and a maximum gain of 1 dBi at 1.7 GHz. For the second band, the impedance bandwidth is from 2.4 GHz to 2.7 GHz allowing for a total bandwidth of 300 MHz. For this band, the minimum peak realized gain is -1.3 dBi at 2.4 and a maximum peak realized gain of 1.3 dBi at 2.6 GHz. The third band extends from 3.15 GHz to 3.5 GHz allowing for a bandwidth of 350 MHz, the minimum peak realized gain is -0.7 dBi at 3.15GHz and a maximum gain of 1.5 dBi at 3.41 GHz. The fourth band extends from 4.4 GHz to 4.5 GHz allowing for a bandwidth of 100 MHz, the minimum peak realized gain is 1.3 dBi at 4.5 GHz and a maximum gain of 1.7 dBi at 4.42 GHz For the final 5th band, the bandwidth of 750 MHz is located between 5.15 GHz to 5.9 GHz. The maximum peak realized gain in this band is 2.9 dBi at 5.65 GHz and the minimum is 1.5 dBi at 5.15 GHz. Simulated peak gain for both the antennas in the lower band is low compared to the antenna gain in the upper band due to the small electrical size of the antenna in the lower band of operation. This describes that the gain is directly proportional to the size of the antenna.

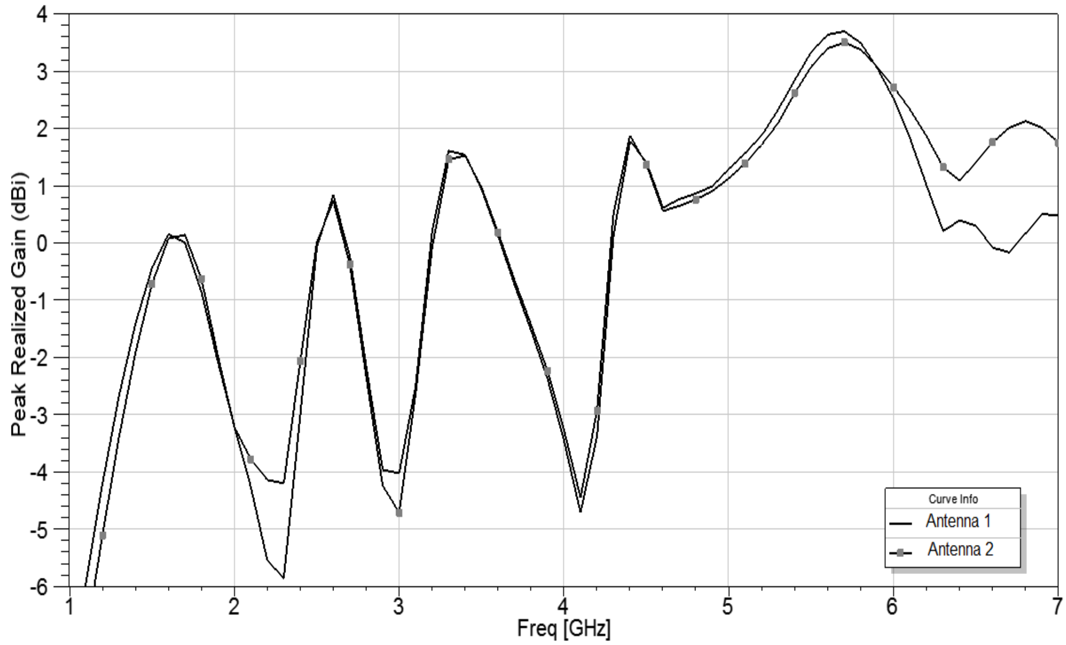

Figure 5.12. Variation of peak realized gain vs. frequency with a -6 dB criteria for two element design for case1.

5.4.4 Radiation Patterns

The simulated 2D and 3D radiation patterns for both the antennas at center frequencies of the operating bands. Where the results belong to antenna no.1 (Figures 5.13) and antenna no.2 (Figures 5.14) being excited separately. Figures 5.13 (a-d) show the 2D co-polarization and cross polarization realized gain radiation patterns for the XZ and the YZ planes for antenna no.1 excited and antenna no.2 connected to a 50 ohms load for 1.6 GHz, 2.55 GHz, 3.3 GHz and 5.5 GHz. The related 3-D radiation patterns are also shown in Figure 5.13 these patterns demonstrate a semi omni-directional radiation pattern that is suitable for a hand held wireless devices as shown in Figure 4.13.

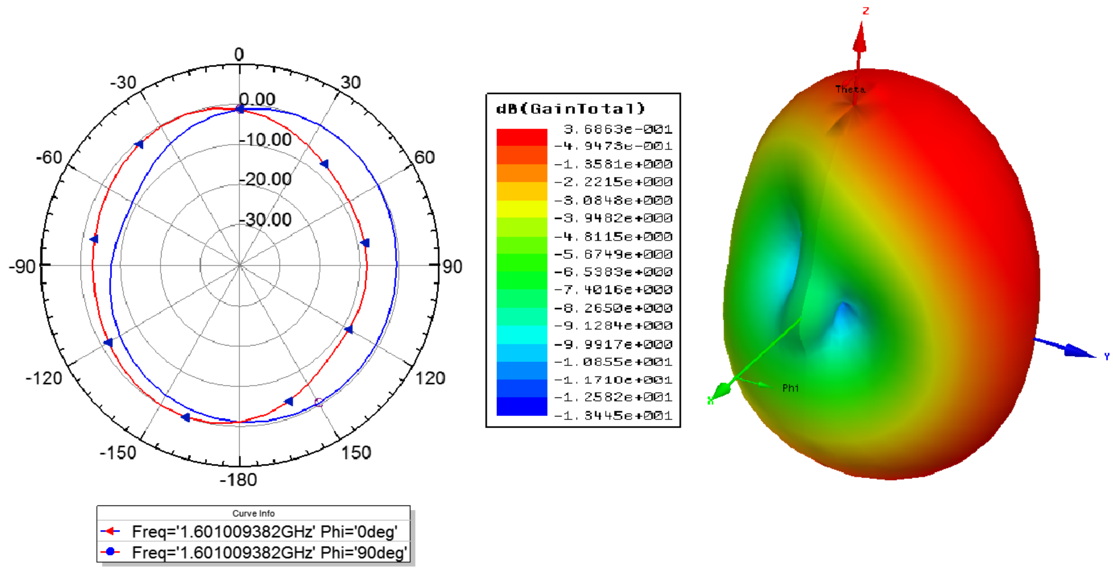

0
30
60
90
120
150
-180
-150
-120
-90
-60
-30
0.00
-10.00
-20.00
-30.00
Curve Info
Freq='1.601009382GHz' Phi='0deg'
Freq='1.601009382GHz' Phi='90deg'
dB(GainTotal)
3.6863e-001
-4.9473e-001
-1.3581e+000
-2.2215e+000
-3.0848e+000
-3.9482e+000
-4.8115e+000
-5.6749e+000
-6.5383e+000
-7.4016e+000
-8.2650e+000
-9.1284e+000
-9.9917e+000
-1.0855e+001
-1.1718e+001
-1.2582e+001
-1.3445e+001
Z
Theta
Y
Phi
X

(a)

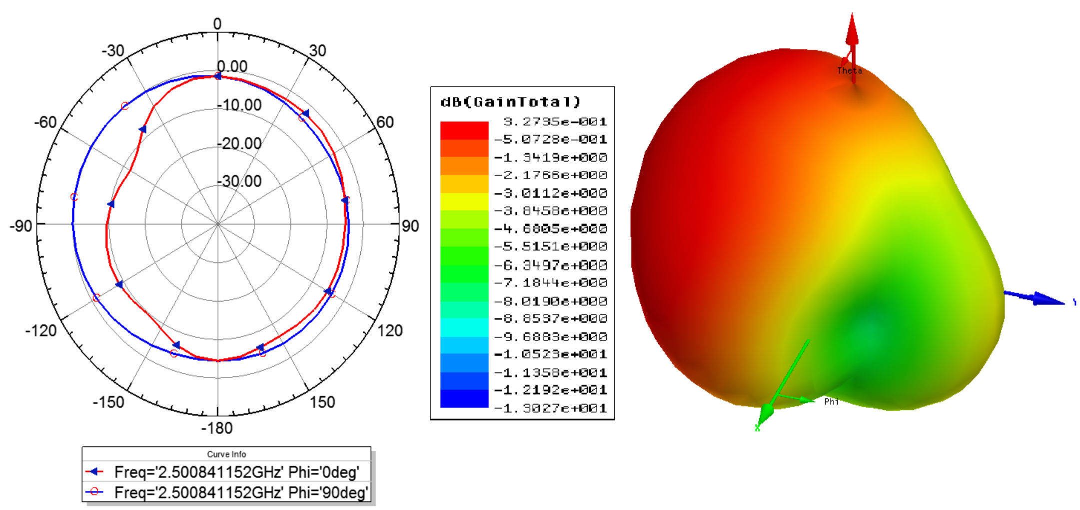

0
30
60
90
120
150
-180
-150
-120
-90
-60
-30
0.00
-10.00
-20.00
-30.00
Curve Info
Freq='2.500841152GHz' Phi='0deg'
Freq='2.500841152GHz' Phi='90deg'
dB(GainTotal)
3.2735e-001
-5.0728e-001
-1.3419e+000
-2.1766e+000
-3.0112e+000
-3.8458e+000
-4.6805e+000
-5.5151e+000
-6.3497e+000
-7.1844e+000
-8.0190e+000
-8.8537e+000
-9.6883e+000
-1.0523e+001
-1.1358e+001
-1.2192e+001
-1.3027e+001
Theta
Phi

(b)

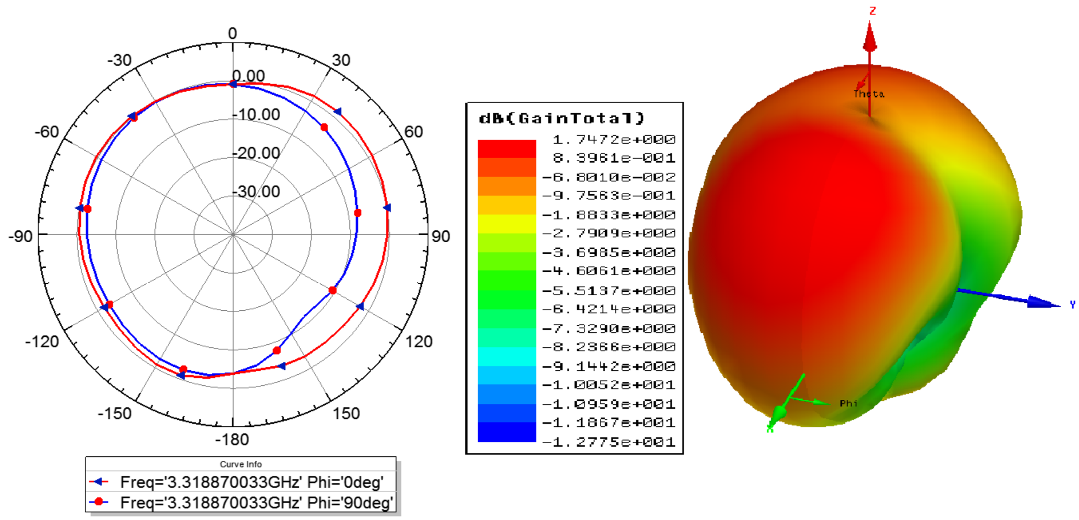

(c)

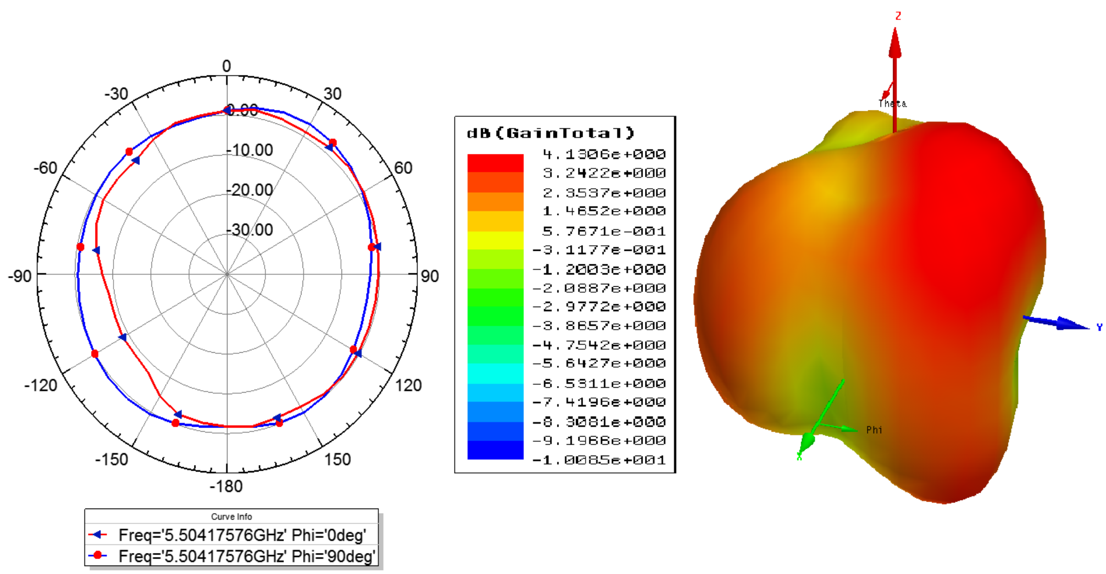

(d)

Figure 5.13. Simulated radiation pattern of antenna no.1 at (a) 1.6 GHz, (b) 2.55 GHz, (c) 3.3 GHz, and (d) 5.5 GHz for case1.

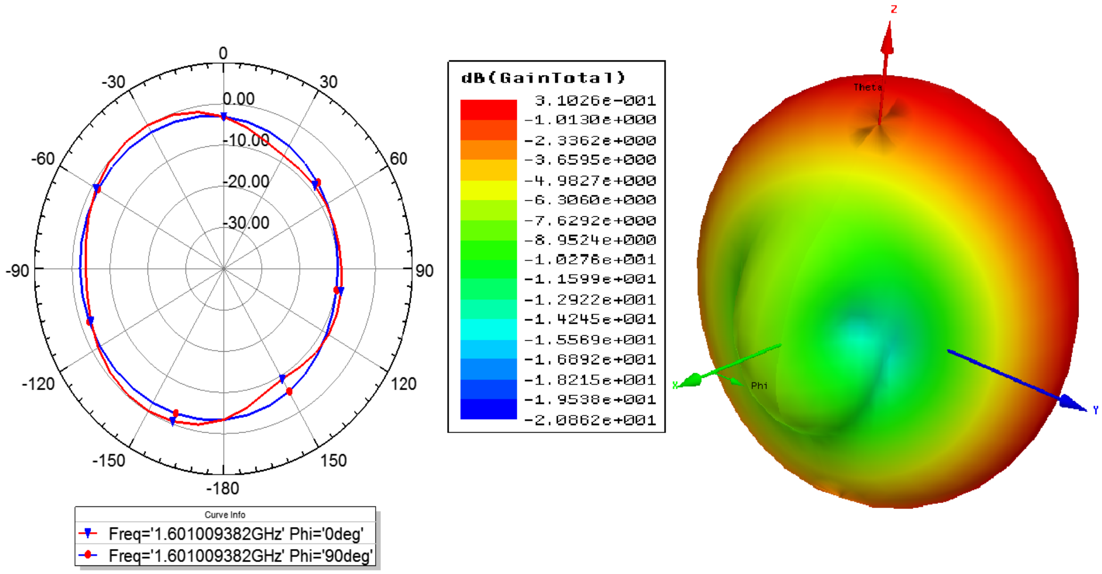
0
30
60
90
120
150
-180
-150
-120
-90
-60
-30
0.00
-10.00
-20.00
-30.00
Curve Info
Freq='1.601009382GHz' Phi='0deg'
Freq='1.601009382GHz' Phi='90deg'
dB(GainTotal)
3.1026e-001
-1.0130e+000
-2.3362e+000
-3.6595e+000
-4.9827e+000
-6.3060e+000
-7.6292e+000
-8.9524e+000
-1.0276e+001
-1.1599e+001
-1.2922e+001
-1.4245e+001
-1.5569e+001
-1.6892e+001
-1.8215e+001
-1.9538e+001
-2.0862e+001
Z
Theta
Phi
X
Y

(a)

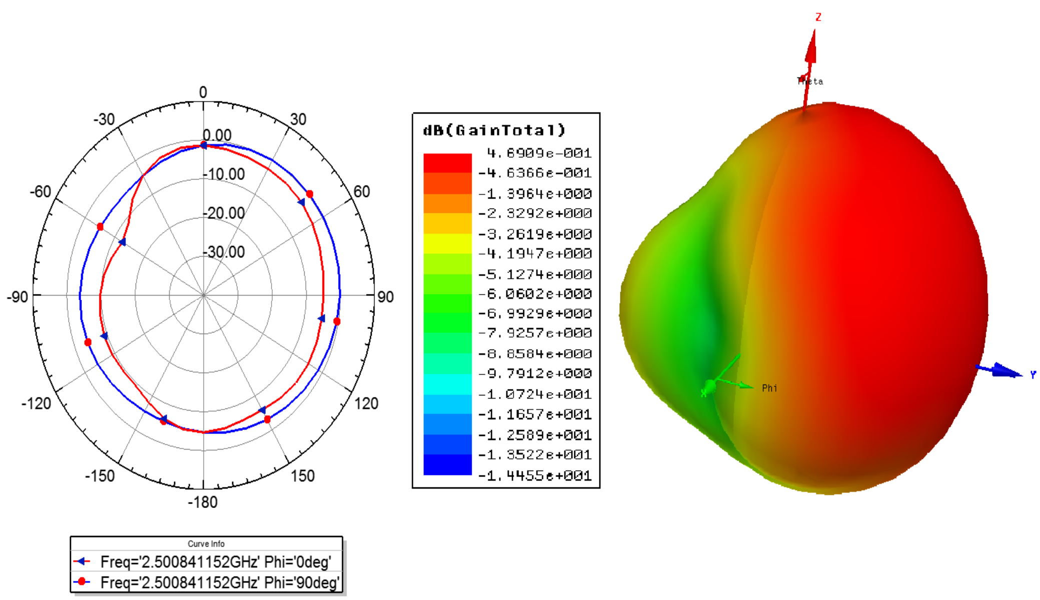
0
30
60
90
120
150
-180
-150
-120
-90
-60
-30
0.00
-10.00
-20.00
-30.00
Curve Info
Freq='2.500841152GHz' Phi='0deg'
Freq='2.500841152GHz' Phi='90deg'
dB(GainTotal)
4.6909e-001
-4.6366e-001
-1.3964e+000
-2.3292e+000
-3.2619e+000
-4.1947e+000
-5.1274e+000
-6.0602e+000
-6.9929e+000
-7.9257e+000
-8.8584e+000
-9.7912e+000
-1.0724e+001
-1.1657e+001
-1.2589e+001
-1.3522e+001
-1.4455e+001
Z
Phi
Y

(b)

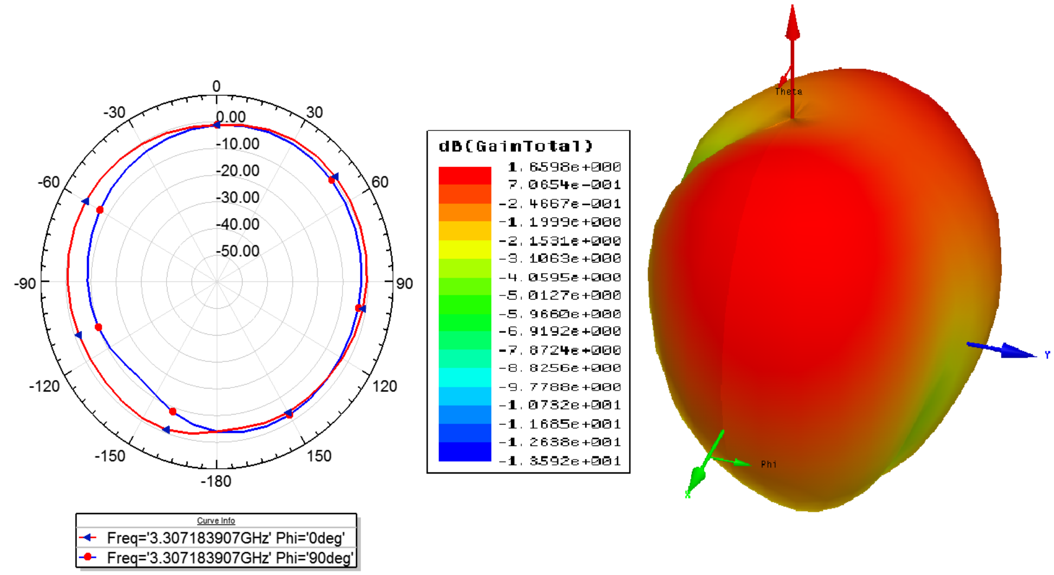

(c)

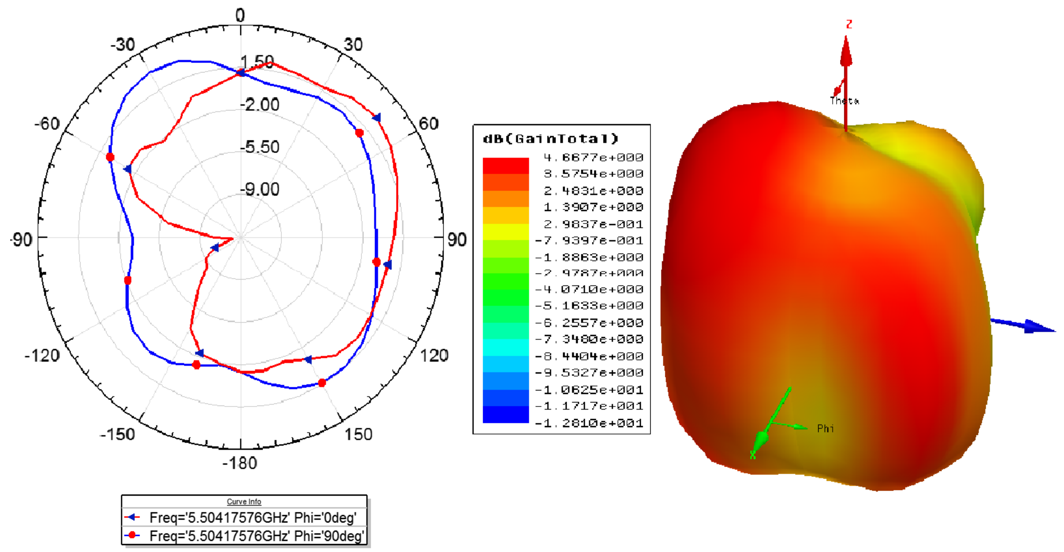

(d)

Figure 5.14. Simulated radiation pattern of antenna no.2 at (a) 1.6 GHz, (b) 2.55 GHz, (c) 3.3 GHz, and (d) 5.5 GHz for case1.

The results that follow below are for antenna no.2. Figures 5.14 (a-d) show the 2D co-polarization and cross polarization realized gain radiation patterns for the XZ and the YZ planes with antenna 2 excited and antenna 1 connected to a 50 ohms load for 1.6 GHz, 2.55 GHz, 3.3 GHz and 5.5 GHz. The related 3-D radiation patterns are also shown in Figure 5.14 these patterns demonstrate a nearly omni-directional radiation pattern that is suitable for a hand held wireless devices.

5.4.5 Current Distribution:

Figure 5.15 and figure 5.16 show the current distributions of simulated MIMO antenna configuration of case 1 for antenna no.1 and antenna no.2. Its clearly seen that current is mainly concentrated on the loop pattern strip and some current on the ground plane, it also seen that when one of the two elements is excited, a weak current is induced in the other element in the non-excited element, which mean that low correlation between two antenna of the MIMO configuration.

5.5 Diversity Performance Evaluation

The diversity performance of the proposed multi-element antenna is calculated in this section. The diversity performance has been evaluated by calculating the envelope correlation coefficient and diversity gain of the antennas.

5.5.1 Envelope Correlation Coefficient

The envelope correlation coefficient has been calculated from S-parameters using equation (3.8). Figure 5.17 shows ECC plot, the figure shows that in all the frequency bands the ECC values of the proposed antenna are lower than 0.5, this value suitable for the design of MIMO configuration in handheld devices.

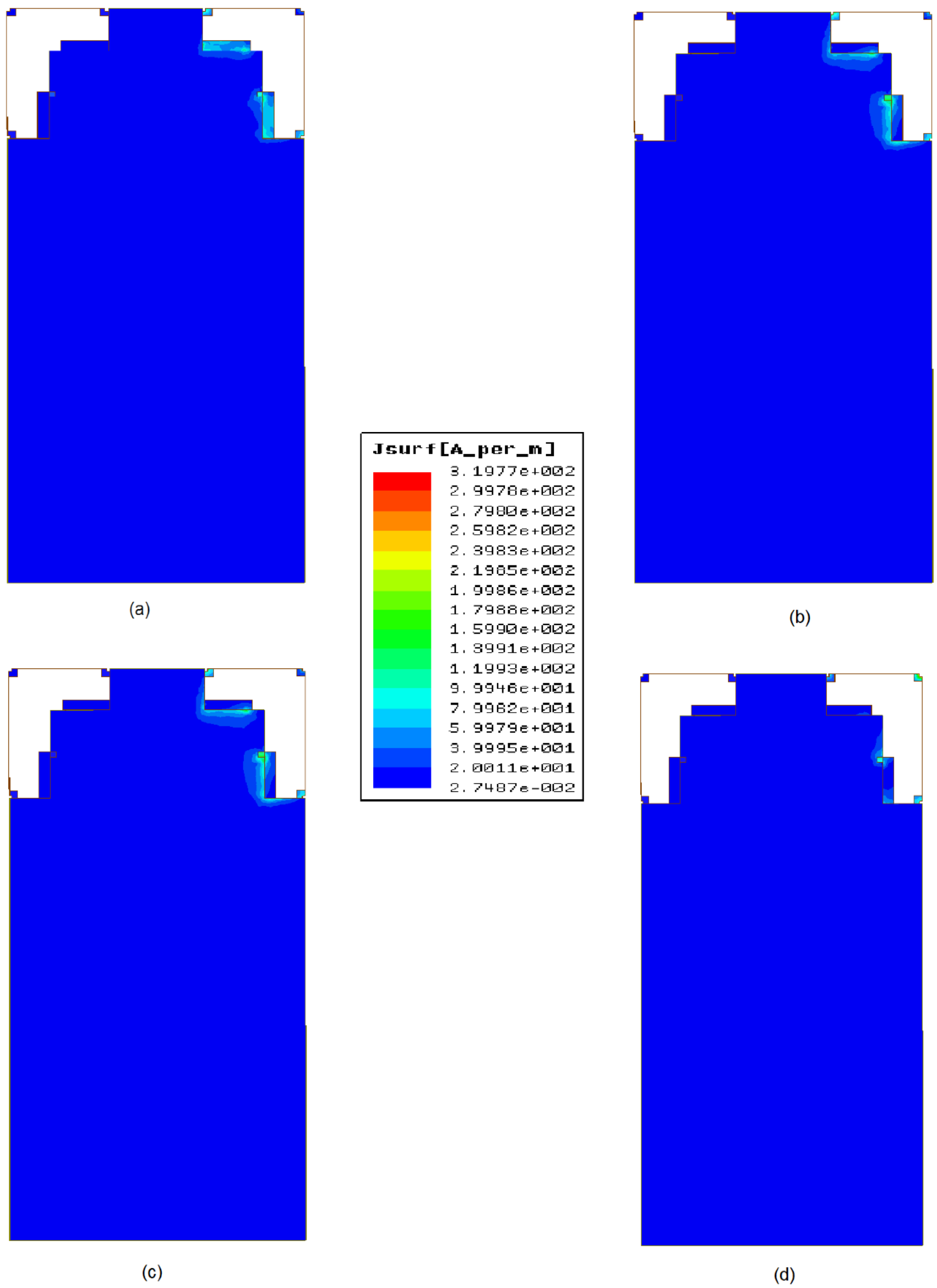

Figure 5.15. Simulated surface current distributions at centre resonant frequencies of the four resonant modes for the antenna no.1 for case1 with the system ground plane at (a) 1.6GHz, (b) 2.55 GHz, (c) 3.3GHz, and (d) 5.5 GHz

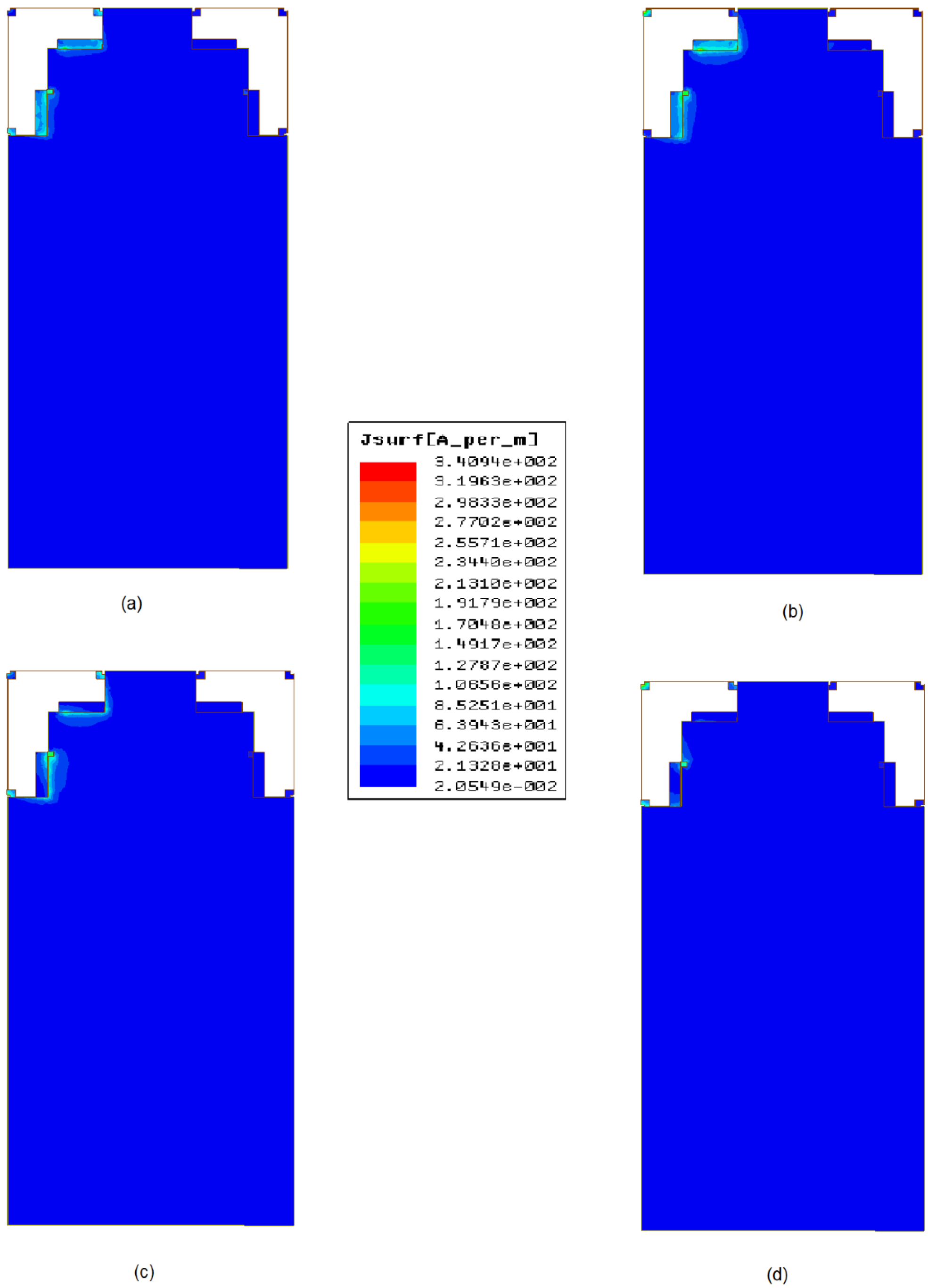

Figure 5.16. Simulated surface current distributions at center resonant frequencies of the four resonant modes for the antenna no.2 for case1 with the system ground plane at (a) 1.6GHz, (b) 2.55 GHz, (c) 3.3GHz, and (d) 5.5 GHz

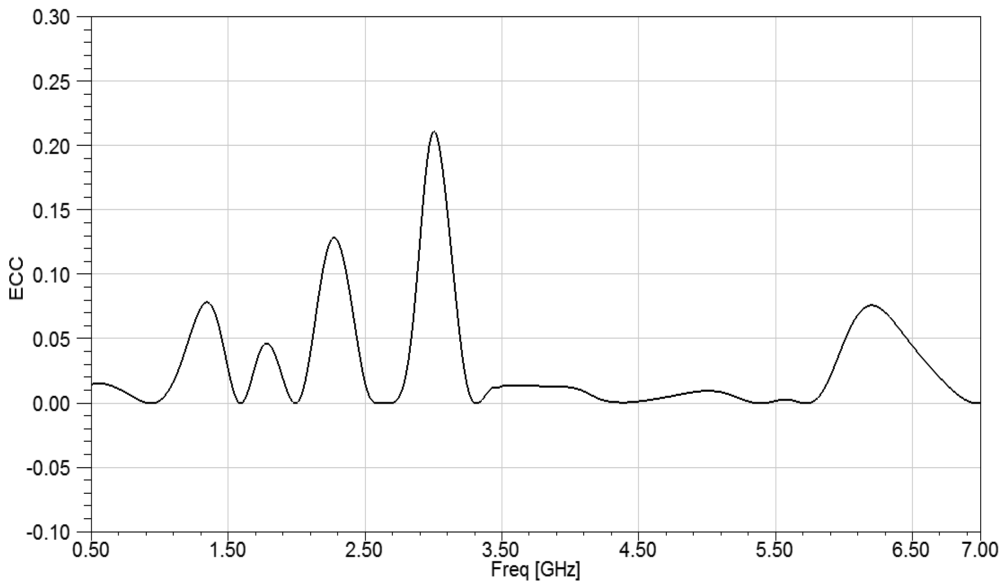

Figure 5.17. Simulated envelope correlation for the MIMO configuration for case1.

5.5.2 Diversity Gain

Diversity gain of the proposed multiple antenna has been calculated from correlation coefficient using equation (3.14) and (3.15). Apparent diversity gain and effective diversity gain are shown in figure 5.18 and figure 5.19. The apparent diversity gain values are higher than 10 dB over all mentioned frequency bands and it gives the good performance of MIMO system. Effective diversity gain values are higher than 8 dB over all mentioned frequency bands. The simulated diversity gain result of the proposed dual-element FLA MIMO agree with the theoretical diversity gain of 10dB for the case of dual-element antenna system in selection combining.

Table 5.1 shows the summary of the simulation results includes the impedance bandwidth, peak gain and correlation coefficient. The results shown is based on the reflection coefficient level -6 dB criteria.

Table 5.1. Parameters evaluation of the proposed antenna.

Center Frequency	Frequency range	Bandwidth (MHz)	Gain	ECC
1.6 GHz	1.39 –1.82GHz	430	1 dBi	0.05
2.6 GHZ	2.4 – 2.7 GHz	300	1.3 dBi	0.02
3.3 GHz	3.15 – 3.5 GHz	250	1.5 dBi	0.02
5.6 GHz	5.15-5.9 GHz	750	2.9 dBi	0.05

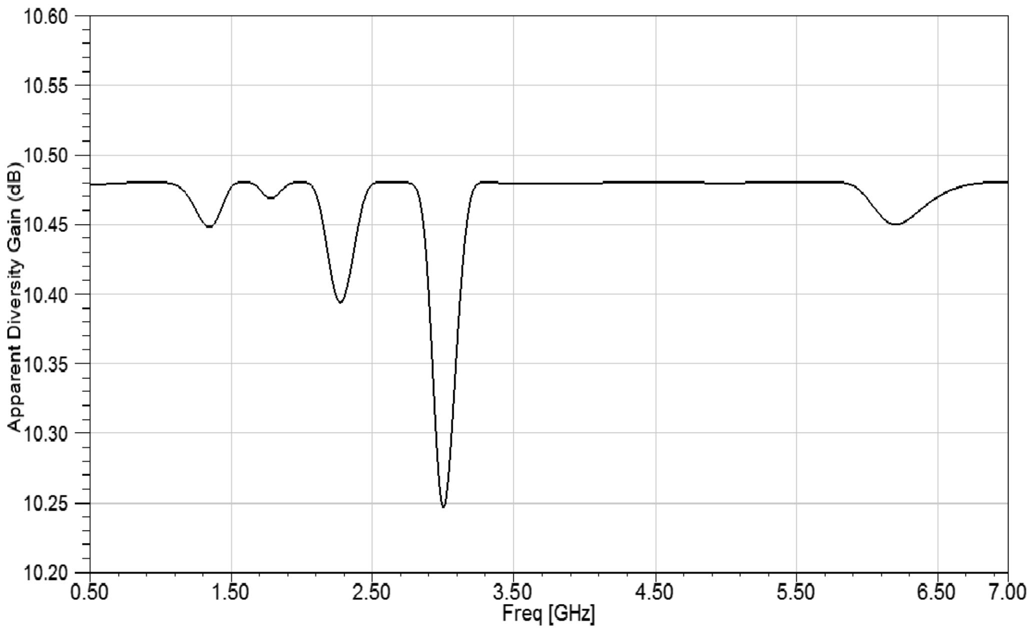

Figure 5.18. Simulated apparent diversity gain for the MIMO configuration for case1

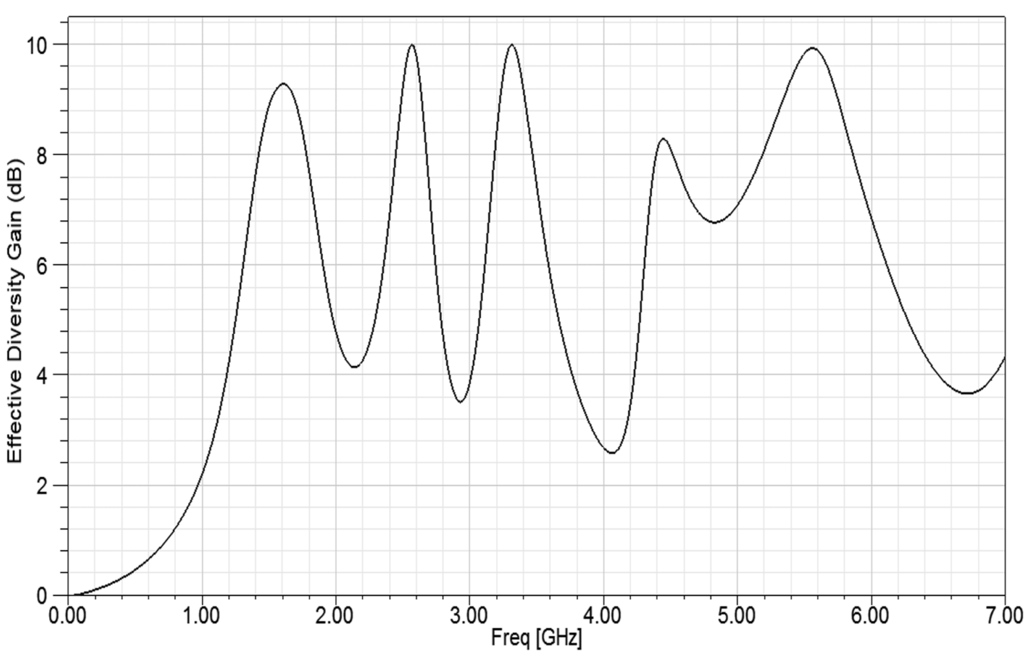

Figure 5.19. Simulated effective diversity gain of the MIMO configuration for case 1.

5.6 Summary

In this chapter, a deployment of MIMO configuration of the FLA antenna was studied. Three different configuration of multiple antenna placement on the ground plane are investigated to compare the results in terms of return loss, mutual coupling and correlation coefficients. Simulation results of the proposed multiple element antenna design were presented. Antenna performance parameters such as the reflection coefficient, mutual coupling, peak realized gain, envelope correlation, current distributions and 2D/3D radiation patterns were studied. The results meet all the required specification where low correlation coefficient and high effective diversity gain are obtained. Table 4.1 was also given to summarize the antenna performance results.

6

Conclusion and Future Work

6.1 Conclusion

The topic of this thesis was to design and investigate a compact folded loop multiband antenna for 4G LTE targeted for MIMO applications. Folded loop is chosen as a radiating element as this antenna could be built with a very small occupied volume by forming in a folded structure, achieving small and low profile. In addition as the antenna structure results very less currents on the ground plane, makes folded loop antenna appropriate for use in the design of multiple antennas on a small mobile terminal as low correlation between the antennas could be achieved. Also the loop antenna has the ability to operate at multiple frequency bands simultaneously.

The background and a brief introduction to multiple antennas techniques were introduced in Chapter 2. Parameters like envelope correlation, diversity gain and efficiency were discussed. The explanation of the steps to calculate the performance metrics of multiple antenna was studied.

A single element dielectric folded loop antenna have been designed the antenna dimension suitable for dimension of 110 mm x 50 mm handheld devices size. The parametric analysis were made to get the optimized parameters. The proposed loop antenna generated four impedance bandwidths 1400-1770 MHz, 2400-2700 MHz, 3146-3500 MHz, and 5090-5900 MHz which can be used to cover the multiple LTE/WLAN/WiMAX mobile phone operations, antenna parameters like 2D radiation patterns, 3D radiation patterns and current distributions were examined. Antenna indicates near omni-directional patterns for all the bands.

A MIMO configuration of the FLA was studied. The MIMO antenna was also designed to be suitable to a handheld devices form factor. The point is to design a two element multiple antenna on the same ground plane with lower correlation values while keeping same operating bands and gain. Three different configuration of the two antenna placement on the ground plane was studied to compare the results in terms of return loss, mutual coupling and correlation. The result meet all the required specification where low correlation coefficient and high effective diversity gain are obtained.

6.2 Future Work:

As for the matter of future work, there are several additional studies should be considers as the following:

- Amendment can be done on antenna structure dimensions to improve the antenna impedance bandwidth. For example, trace widths, trace spacing, feed positioning, and overall antenna structure dimensions.
- The two element folded loop antenna was considered for a handheld terminal, therefore, the user's effect on the multiple antenna's performance should be studied, hearing aid compatibility (HAC) could be evaluated.
- The Specific Absorption Rate (SAR) value inside the user's head caused by the antenna arrays should also be considered.
- The channel capacity of the two element FLA could be investigated in several environments such as the outdoor and indoor environments.
- The antenna simulation model did not mounted inside a mobile phone, the performance and behavior of antenna in the presence of mobile components such as screen, case and other components should be considered.

References

[1] M. S. Sharawi, "Printed multi-band MIMO antenna systems and their performance metrics," IEEE Antennas and Propagation Magazine, vol. 55, no. 5, pp. 218-232, 2013.

[2] G. J. Foschini, and M. J. Gans, "On limits of wireless communications in a fading environment when using multiple antennas," Wireless Personal Communications, vol. 6, pp. 311-335, 1998.

[3] D. Gesbert, M. Shafi, D. Shiu, P. J. Smith and A. Naguib, "From theory to Practice: An overview of MIMO space-time coded wireless systems," IEEE Jrnl. on Select. Areas Comm., vol. 21, no. 3, pp. 281-302, 2003.

[4] 3GPP Technical Specification Group, "Spatial channel model, SCM-134 text V6.0," Spatial Channel Model AHG (Combined as-hoc from 3GPP and 3GPP2), Apr. 2003.

[5] V. Erceg et.al., "IEEE 802.16 Broadband Wireless Access Working Group," IEEE 802.16.3c-01/29r4, http://ieee802.org/16, 2001.

[6] A. N. Kulkarni, "Investigation on compact antenna solutions for future 4G LTE wireless devices with MIMO implementation," M.S. thesis, Dept. Elect. Eng., San Diego State University, San Diego, 2012.

[7] H. Rohil, P. Mutreja and S. Kumar, "A comparative analysis of WiMAX and Wi-Fi," International Journal of Research in IT, Management and Engineering, vol. 1, issue 2, pp. 144-158, 2011.

[8] S. Sesia, I. Toufik, and M. Baker, "LTE—The UMTS Long Term Evolution:From Theory to Practice," Wiley, Chichester, U.K, 2009.

[9] M. Han and J. Choi, "Small-size printed strip MIMO antenna for next generation mobile handset application,"Microw. Opt. Technol. Lett., vol. 53, no. 2, pp. 348-352, 2011.

[10] C. Dai, D. Wu, and Y. Wu, "Design of an internal multi-band loop antenna for multiple mobile handset operations," IEEE International Wireless Symposium (IWS), pp.1-4, 2013.

[11] M. Zheng, and H. Y. Wang, “Internal hexa-band folded monopole/dipole/loop antenna with four resonances for mobile device,” IEEE Trans. Antennas Propag., vol. 60, pp. 1–6, 2012.

[12] W. Y. Li and K. L. Wong, “Surface-mount loop antenna for WWAN/WLAN/ WiMAX operation in the mobile phone,” Asia Pacific Microwave Conference (APMC 2008), pp. 1–4, 2008.

[13] C.-W. Chiu and Y.-J. Chi, “Printed loop antenna with a u-shaped tuning element for hepta-band laptop applications,” IEEE Trans. Antennas Propag., vol. 58, no. 11, pp. 68-71, 2010.

[14] C.-W. Chiu and C.-H. Chang, “Multiband folded loop Antenna for smart phones,” Progress In Electromagnetics Research, PIER 102, pp. 213-226, 2010.

[15] L. Mouffok, A. C. Lepage, J. Sarrazin, “A compact dual-band dual-port diversity antenna for LTE,” Advanced Electromagnetics, vol. 1, no. 1, 2012.

[16] S. W. Su, “High-gain dual-loop antennas for MIMO access points in the 2.4/5.2/5.8 GHz bands,” IEEE Trans. on Antenna and Propaga., vol. 58, pp. 2412–2419, 2010.

[17] H. Li, J. Xiong, and S. He, “A compact planar MIMO antenna system of four elements with similar radiation characteristics and isolation structure,” IEEE Antennas and Wireless Propaga. Lett., vol. 8, pp.1107–1110, 2009.

[18] ANSYS HFSS, Ansys Inc, URL http://www.ansys.com/Products/Simulation+ Technology/Electronics/Signal+ Integrity/ANSYS+HFSS/Features.

[19] P. Dhande “Antennas and its Applications,” DRDO Science Spectrum, pp. 66-78, 2009.

[20] J. D. Kraus and R. J. Marhefka, Antennas for all Applications, 3rd ed., New York: McGraw-Hill, 2002.

[21] D. M. Pozar, Microwave Engineering, 2nd ed., John Wiley and Sons, Inc., New York, 1998.

[22] IEEE Transactions on Antennas and Propagation, Vols. AP-17, No. 3, May 1969; Vol. AP-22, No. 1, January 1974; and Vol. AP-31, No. 6, Part II, November 1983.

[23] C. A. Balanis, Antenna Theory: Analysis and Design, John Wiley and Sons, Inc., New York, 2005

[24] D. M. Pozar, Microwave and RF Design of Wireless System, Wiley, New York, 2001.

[25] C.-C. Lin, L.-C. Kuo, and H.-R. Chuang, "A horizontally polarized omnidirectional printed antenna for WLAN applications," IEEE Transactions on Antennas and Propagation", vol. 54, no.11, pp. 3551-3556, 2006.

[26] W. Geyi, Q. Rao, S. Ali and D. Wang "Handset antenna: practice and theory," Progress in Electromagnetics Research, vol. 80, pp. 23–160, 2008.

[27] Y. W. Chi and K. L. Wong, "Internal compact dual-band printed loop antenna for mobile phone application," IEEE Transaction Antennas Propagation, vol. 55, pp. 1457–1462, 2007.

[28] B. Jung, H. Rhyu, Y. J. Lee, F. J. Harackiewwicz, M. J. Park, and B. Lee, "Internal folded loop antenna with tuning notches for GSM/GPS/ DCS/PCS mobile handset applications," Microwave Optical Technology. Letters, vol. 48, pp. 1501–1504, 2006.

[29] W. Y. Li and K. L. Wong, "Surface-mount loop antenna for amps/GSM/DCS/ PCS operation in the mobile phone," Microwave Opt. Technol. Letters, vol. 49, pp. 2250–2254, 2007.

[30] M. Hunynh and W. Stutzman, "Ground plane effects on planar inverted-F antenna (PIFA) performance," IEEE Proc. Microwave Antennas Propagation, vol. 150, no. 4, pp. 209-213, 2003.

[31] M. F. Abedin and M. Ali, "Modifying the ground plane and its effect on planar inverted-F antennas (PIFAs) for mobile phone handsets," IEEE Antennas Wireless Propagation. Letter, vol. 2, No. 15, pp. 226-229, 2003.

[32] H. Morishita, Y. Kim, and K. Fujimoto, “Design concept of antenna for small mobile terminals and the future perspective," IEEE Transactions on Antennas and Propagation, vol. 55, no. 5, pp. 30-43, 2002.

[33] P. J. Vainikainen, Ollikainen, O. Kivekas, and K. Kelander, “Resonator-based analysis of the combination of mobile handset antenna and chassis,” IEEE Transactions on Antennas and Propagation, vol. 50, no. 10, pp.1433-1444, 2002.

[34] H. Morishita, Y. Kim, Y. Koyanagi and K. Fujimoto, “A folded loop antenna system for handsets,” IEEE AP-S Proc., vol. 3, pp. 440-443, 2001.

[35] Y. Kim, H. Morishita, Y. Koyanagi and K. Fujimoto, “A folded loop antenna system for handsets developed and based on the advanced design concept,” IEICE Trans. Communication, vol. E84- B, no. 9, pp. 2468-2475, Sept 2001.

[36] K. L. Wong, Planar Antennas for Wireless Communications,” New York: Wiley, 2003.

[37] L. Zheng and D.N.C. Tse. “Diversity and multiplexing: a fundamental tradeoff in multiple-antenna channels,” IEEE Transaction on Information Theory, vol.49, no. 5, pp.1073–1096, 2003.

[38] S. Nema and S. Gaikwad, “MIMO technology for wireless sensor Network,” International Journal of Computer Science & Communication Networks, vol. 1, issue 2, pp.105-110, 2011.

[39] S. M. Alamouti, “A simple transmit diversity technique for wireless communications,” IEEE J. Select. Areas Commun., vol. 16, pp.1451–1458, Oct. 1998

[40] F. DeFlaviis, L. Jofre, J. Romeu, and A. Grau, “Multiple Antenna System for MIMO Communications,” San Rafael, CA, Morgan & Claypool Publishers, 2008.

[41] I. E. TELATAR, “Capacity of multiantenna Gaussian channels”, European Transactions on Telecommunications, vol. 10, no. 6, pp. 585–595, 1999

[42] J. D.Gibson, The Communication Handbook, 2nd ed. CRC Press, 2002.

[43] C. C. Chiau, “Study of the diversity antenna array for the MIMO wireless communication systems," Ph.D. thesis, Queen Mary University, 2006.

[44] K. Hirasawa and M. Haneishi, “Measurement of small and low-profile antennas”, Artech House, 1992.

[45] P. Irazoqui-Pastor, J. T. Bernhard, “Examining the performance benefits of antenna diversity systems in portable wireless environments,” IEEE Antenna Applications Symposium, Allerton Park, 1999.

[46] R. G. Vaughan, “Polarization diversity in mobile communications,” IEEE Transactions on Vehicular Technology, vol. 39. no.3, pp. 177-185, 1990.

[47] P. W. Raut And Dr. S.L. Badjate, “Diversity techniques for wireless communication,” International Journal of Advanced Research in Engineering & Technology (IJARET), vol. 4, Issue 2, pp.144–160, 2013

[48] N. Srivastava, “Diversity schemes for wireless communication- A short review”, Journal of theoretical and applied information technology, Islamabad, Pakistan, vol. 15. no.2, issue 31, 2010.

[49] T. S. Rappaport, Wireless Communications, Principles and Practice, 2nd Edition, Pearson Education, Upper Saddle River, NJ, 2002.

[50] B. Guo, “Antenna diversity in mobile phone”, M.S. thesis Chalmers University of Technology, 2008

[51] F. Adachi, M. T. Feeney, A. G. Willianson, J.D. Parsons, “Cross correlation between the envelopes of 900MHz signals received at a mobile radio base station site,” IEE Proceedings Radar and Signal Processing, vol. 133, no .6, pp 506-512,1986.

[52] M. Jensen and Y. Rahmat-Samii, “Performance analysis of antennas for hand-held transceivers using FDTD,” IEEE Trans. on Antennas and Propagation, vol. 42, no. 8, pp. 1106-1113, 1994.

[53] R. H. Clarke, “A Statistical Theory of Mobile Radio Reception”, Bell System Technical Journal, pp. 957-1000, 1966.

[54] S. Blanch, J. Romeu and I. Corbella, "Exact representation of antenna system diversity performance from input parameter description," Electronics Letters 1st vol. 39 no. 9, pp. 705-707, 2003.

[55] K. Karlsson, "Embedded Element Patterns in Combination with Circuit Simulations for Multi-Port Antenna Analysis", Ph.D. thesis, Chalmers University of Technology, Sweden, Oct. 2, 2009.

[56] M. Hashemi, "Designing feeding network for multi-band MIMO antenna", M.S. thesis, Chalmers University of Technology, Sweden, 2010.

[57] P. S. Kildal, Foundations of Antennas, Compendium in Antenna Engineering at Chalmers, 2009.

[58] A. Hussain, U. Carlberg, J. Carlsson, and P. S. Kildal, "Analysis of statistical uncertainties involved in estimating ergodic MIMO capacity and diversity gain in Rayleigh fading environment," ICECom, 2010 Conference Proceedings, pp. 1-4, 2010.

[59] W. L. Stutzman, and G. A. Thiele, Antenna Theory and Design, 2nd edition, John Wiley & Sons, Inc., 1998.